



Depósito de investigación de la Universidad de Sevilla

<https://idus.us.es/>

"This document is the Accepted Manuscript version of a Published Work that appeared in final form in Journal of the American Chemical Society, copyright © American Chemical Society after peer review and technical editing by the publisher. To access the final edited and published work see <https://doi.org/10.1021/jacs.2c09471> ."

Ethylene Dimerization and Oligomerization Using Bis(phosphino)boryl Supported Ni Complexes

Fanji Kong^{†1}, Pablo Ríos^{†2}, Conner Hauck¹, Francisco José Fernández-de-Córdova², Diane A. Dickie¹, Laurel G. Habgood³, Amor Rodríguez^{2*} and T. Brent Gunnoe^{1*}

[†]These authors contributed equally to this work.

¹Department of Chemistry, University of Virginia; Charlottesville, Virginia 22904, United States.

²Instituto de Investigaciones Químicas (IIQ), Department of Inorganic Chemistry CSIC and University of Seville, Center for Innovation in Advanced Chemistry (ORFEO-CINQA), C/Américo Vespucio 49, Seville, 41092, Spain.

³Department of Chemistry, Rollins College, Winter Park, Florida 32789, United States.

*Corresponding author. Email: tbg7h@virginia.edu

*Corresponding author. Email: marodriguez@iiq.csic.es

Abstract

We report the dimerization and oligomerization of ethylene using bis(phosphino)boryl supported Ni(II) complexes as catalyst precursors. By using alkylaluminum(III) compounds or other Lewis acid additives, Ni(II) complexes of the type (^RPBP)NiBr (R = *t*Bu or Ph) show activity for the production of butenes and higher olefins. Optimized turnover frequencies of 640 mol_{ethylene}·mol_{Ni}⁻¹·s⁻¹ for the formation of butenes with 41(1)% selectivity for 1-butene using (^{Ph}PBP)NiBr, and 68 mol_{ethylene}·mol_{Ni}⁻¹·s⁻¹ for butenes production with 87.2(3)% selectivity for 1-butene using (^{*t*Bu}PBP)NiBr, have been demonstrated. With methylaluminoxane as co-catalyst and (^{*t*Bu}PBP)NiBr as the precatalyst, ethylene oligomerization to form C₄ through C₂₀ products was achieved while the use of (^{Ph}PBP)NiBr as the pre-catalyst retained selectivity for C₄ products. Combined experimental and computational studies indicate that the ethylene dimerization is not

initiated by Ni hydride or alkyl intermediates. Rather, our studies point to a mechanism that involves a cooperative B/Ni activation of ethylene to form a key 6-membered borametallacycle intermediate. Thus, a cooperative activation of ethylene by the Ni–B unit of the (^RPBP)Ni catalysts is proposed as a key element of the Ni catalysis.

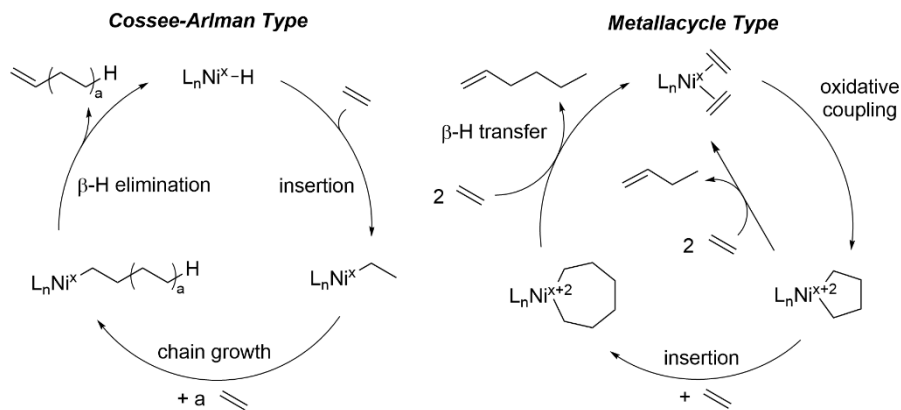
Introduction

Catalytic oligomerization of ethylene is an important commercial method for the production of linear α -olefins (LAOs), which have extensive uses in fuel, petro-, and fine chemistry.¹⁻⁴ Each year, > 3.5 million tons of LAOs are produced globally, and the annual growth rate of world consumption of LAOs forecasted to be approximately 4% during the 2019–2024 period.^{5,6} Since the first discovery of the "nickel effect" by Ziegler and Holzkamp in the 1950s,⁷ the field of nickel catalyzed olefin oligomerization has become one of intense study. Thus, the development of new catalysts for Ni-catalyzed olefin oligomerization and studies of the reaction mechanisms continue to be of interest to academia and industry.⁸⁻¹⁰ Another important milestone in this field was the development of the bidentate P–O ligated Ni complex by Keim and coworkers,¹¹ which ultimately led to the commercialization of the Shell higher olefin process (SHOP) that is used for the production of over one million tons of α -olefins every year.^{2,12-13} This success has encouraged recent studies with the goal of pursuing novel ligand structures to develop new fundamental understanding of how ligand/catalyst structure can impart new types of reactivity.¹²

The generally accepted mechanism for Ni-mediated ethylene oligomerization (*e.g.*, the Shell Higher Olefin Process) is the Cossee-Arlman mechanism (**Scheme 1**, left)^{5,9,14-15} in which the reaction is initiated from a Ni–H/alkyl intermediate followed by ethylene insertion steps (chain growth). The formation of olefin products is generally proposed to occur via β -H elimination from

a Ni-alkyl intermediate followed by net olefin dissociation. Chain propagation is normally controlled by the ratio of ethylene insertion and β -H elimination rates,¹⁰ and frequently Schulz–Flory distributions of ethylene oligomers are obtained.¹⁶⁻¹⁸ Another possible mechanism for Ni-catalyzed ethylene oligomerization involves the formation of a metallacycle similar to the reactions using Cr catalysts,^{9,19} which is normally proposed in the reaction of a Ni pre-catalyst with a Lewis acid activator (*e.g.*, BF_3).²⁰ This type of mechanism has been suggested to be energetically viable based on DFT modeling of phosphine ligated Ni(0) catalyzed ethylene dimerization processes (**Scheme 1**, right).^{2,21} Experimental evidence for a Ni metallacycle mechanism (**Scheme 1**, right) was reported by Grubbs and coworkers using a nickel-based metallacyclopentene complex in the 1970s.²²⁻²⁶

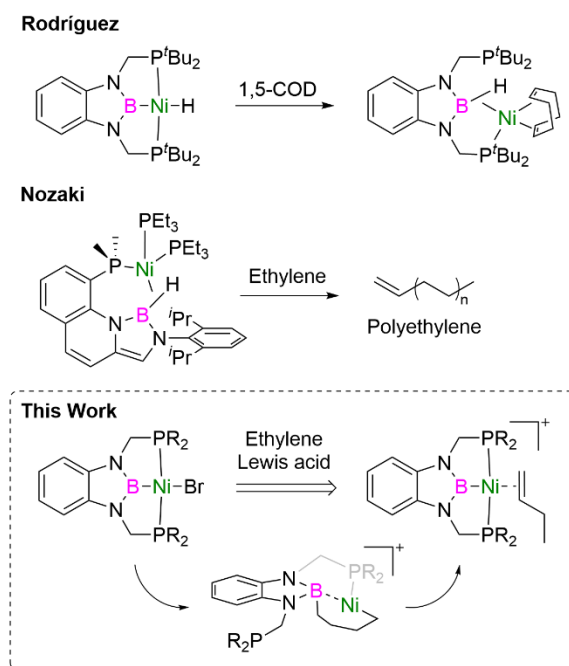
Scheme 1. Proposed mechanisms of Ni-mediated ethylene oligomerization.



Pincer ligands have been widely used in transition-metal-mediated catalysis due, in part, to their tunable steric and electronic properties.²⁷⁻³⁰ As part of the pincer ligand family, examples of bis(phosphino)boryl ligands (^RPBP) have been designed and synthesized by the Nozaki and Yamashita groups,³¹⁻³³ and later, (^RPBP) ligands were studied with transition-metals such as Os,

Ir, Pt, Ru, Rh, Pd and Co.³⁴⁻⁴⁵ Nickel complexes with *t*BuPBP ligands have been isolated and reported to be active for olefin hydrogenation and CO₂ reduction.⁴⁶⁻⁴⁹ In addition, experimental evidence has been reported for the formation of a σ -borane (η^2 -B-H)Ni(0) species from the reaction of (*t*BuPBP)NiH with 1,5-cyclooctadiene, which suggests that the hydride ligand is capable of migration from the Ni center to the boron center (**Scheme 2**).⁵⁰ Recently, the Nozaki group has synthesized a bidentate Ni(0) σ -borane complex $\{(\eta^2$ -B-H/P)Ni $\}$ and demonstrated its application in catalytic polymerization of ethylene for which the (η^2 -B-H/P)Ni complex behaves as a masked Ni(II) boryl hydride that selectively produces linear polyethylene but not lower molecular weight ethylene oligomers (**Scheme 2**).⁵¹ These studies suggest that the installation of a non-innocent boryl-moiety in the ligand structure offers unique reactivity, such as serving as a hydride shuttle, and could potentially alter the reaction pathway for catalytic processes.

Scheme 2. Examples of previously reported reactions of olefins with PBP-Ni and related PB-Ni complexes and this work.



Herein, we report catalytic ethylene oligomerization reactions using a series of (^RPBP)NiBr (R = *t*Bu, Ph, or Cy) catalyst precursors. Unique aspects of these catalytic processes include substantial activities for ethylene dimerization with an Al-based or Lewis acid co-catalysts, tunable selectivity for ethylene dimerization versus oligomerization based on ligand structure and co-catalyst identity, and a proposed catalytic reaction pathway that involves a non-innocent boron center on the ligand moiety and does not involve a Ni–H or Ni–alkyl intermediate, which we believe is a unique mechanism for olefin coupling processes.

Results and Discussion

Initial screening for ethylene dimerization. During the initial screening via *in situ* ¹H NMR spectroscopy, (^{*t*Bu}PBP)NiOAc (**1**), which was synthesized from (^{*t*Bu}PBP)NiMe and CO₂,⁴⁹ was found to catalyze slow dimerization of ethylene to form 1-butene without a co-catalyst at 90 °C using C₆D₆ as the solvent (**Table 1**, entry 1). To test if the acetate group is required for the reaction, (^{*t*Bu}PBP)NiBr (**2**) was used, and no peaks associated with the formation of butenes were observed in the ¹H NMR spectra (**Table 1**, entry 2). However, when using complex **2** in the presence of AgBF₄ as an additive for bromide abstraction, the ethylene dimerization reaction was achieved even at a lower temperature (60 °C) with ~75% selectivity for 1-butene (**Table 1**, entry 3). In an effort to achieve an *in situ* Br/OAc metathesis reaction to form complex **1**, both TIOAc and AgOAc were examined as the additive for the ethylene dimerization reaction using complex **2** (**Table 1**, entry 4). The reaction with TIOAc after 2 days provided < 1 TO (turnover) of 1-butene (**Table 1**, entry 5). Based on these results, it can be concluded that the OAc group is likely not essential for the ethylene dimerization, and we speculated that cationic [(^{*t*Bu}PBP)Ni]BF₄, formed through

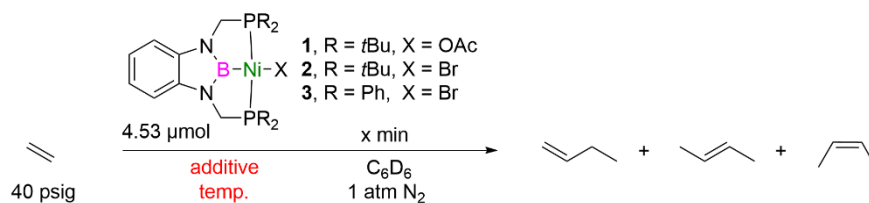
bromide abstraction from **2** with AgBF₄, is likely the active species for the ethylene dimerization reaction. Although we were unable to isolate the cationic complex [(^tBuPBP)Ni][BF₄], a crystal structure of [(^tBuPBP)Ni(OH₂)] [BF₄] was obtained, which likely formed during the month-long crystal growing period in an insufficiently dried solvent (**Figure S42**).

Next, different silver and sodium salts were tested as additives (see Supporting Information, Section 2), and only AgBF₄, AgSbF₆, AgBAR^F and NaBAR^F were found to provide active catalysts for ethylene dimerization in the presence of complex **2** (**Table 1**, entries 3, 6–8). Control experiments using other Ni precursors such as (DME)NiCl₂, NiCl₂ and Ni(OAc)₂ with and without AgBF₄ showed no activity for ethylene dimerization (**Scheme 3A**), which suggests that the ^tBuPBP ligand is important for the dimerization reaction, leading us to speculate about a possible cooperative role for the Ni and B centers in the catalytic mechanism (see below for more discussion on this point).

The Ni(II) complex (^{Ph}PBP)NiBr (**3**) was synthesized and tested for ethylene dimerization, and we found that using **3** as a catalyst precursor yielded butenes at room temperature, but the reaction was less selective for 1-butene (**Table 1**, entries 9–11). It is possible that changing the ^tBu group to a less sterically hindered Ph group on the PBP moiety favors the coordination of 1-butene, which might provide access to a more facile isomerization of 1-butene to 2-butenes compared to the Ni catalyst coordinated by the ^tBuPBP ligand (see below for more discussion and experimental results supporting this suggestion). Propylene was also tested as the substrate using complexes **1–3** in the presence of additives (i.e., AgBF₄, MAO); however, no reaction was observed based on the *in situ* ¹H NMR studies (**Scheme 3B**). We speculate that the dimerization reaction may require the coordination of more than one molecule of ethylene to initiate (see below), and the coordination of two equivalents of propylene seems to be less favorable than ethylene, likely due to sterics,

which would inhibit the dimerization of olefins larger than ethylene. However, a mixture of propylene and ethylene resulted in the formation of higher olefins with an odd number of carbon atoms along with products from ethylene oligomerization. These results indicate the likelihood of a Ni-catalyzed coupling reaction between ethylene and propylene, which also indicates that the coupling of ethylene and other α -olefins, such as 1-butene, is likely possible (see Supporting Information, Section 9). Thus, the Ni-catalysis is selective toward homo-ethylene coupling or ethylene/ α -olefin coupling but is less reactive for the coupling of two α -olefins.

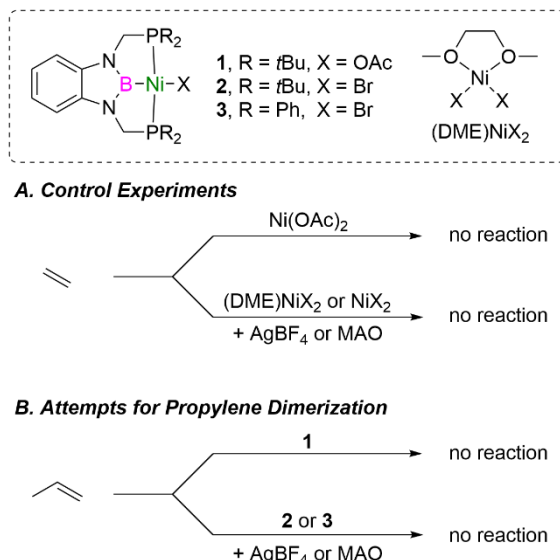
Table 1. Initial attempts for ethylene dimerization using (^RPBP)Ni complexes.^a



Entry	Ni complex	Additive	Time (min)	Temp. (°C)	TOF C_4^b (s^{-1})	1-butene (TOs)	2-butenes (TOs)	
							<i>trans</i>	<i>cis</i>
1	1	none	1440	90	3×10^{-5}	2.3	N.D.	N.D.
2	2	none	240	60	N.D. ^c	N.D.	N.D.	N.D.
3	2	AgBF_4	240	60	1×10^{-4}	1.1	0.24	0.12
4	2	AgOAc	1440	60	N.D.	N.D.	N.D.	N.D.
5	2	TIOAc	2880	60	6×10^{-6}	0.8	N.D.	N.D.
6	2	NaBAr^{F}	240	60	9×10^{-5}	0.5	0.42	0.36
7	2	AgBAr^{F}	240	60	2×10^{-4}	1.3	0.61	0.63
8	2	AgSbF_6	30	r.t.	2×10^{-3}	3.4	0.24	0.28
9	3	AgSbF_6	15	r.t.	1.6×10^{-2}	3.48	6.75	4.42
10	3	AgBF_4	20	r.t.	1.6×10^{-2}	4.92	8.48	5.98
11	3	AgBAr^{F}	30	r.t.	9×10^{-4}	0.56	0.70	0.33

^a Reaction conditions: (^RPBP)NiX (4.53 μmol) in 0.5 mL C_6D_6 , additive (1.0 equiv. relative to Ni pre-catalyst), 40 psig ethylene. ^b TOF $\text{C}_4 = \text{mol}_{\text{butenes}} \cdot \text{mol}_{\text{Ni}}^{-1} \cdot \text{s}^{-1}$. ^c N.D. = not detected.

Scheme 3. (A) Control experiments using other Ni pre-catalysts. (B) Attempts for propylene dimerization using (^RPBP)Ni complexes **1–3**.

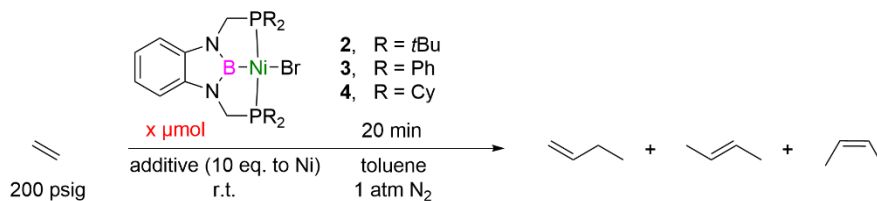


Ethylene dimerization/oligomerization using aluminum co-catalyst. Alkylaluminum compounds have been commonly used as co-catalysts for homogeneous ethylene oligomerization reactions using ligated Ni halide catalyst precursors, which generally led to enhanced activities.^{4,52-56} Therefore, different alkylaluminums were tested as co-catalysts for our (^RPBP)Ni catalysis (**Table 2**), and the resulting rates of ethylene dimerization are improved. Control experiments using (^RPBP)H free ligand, alkylaluminums without Ni, (DME)NiBr₂ with alkylaluminums, and (^RPBP)H free ligand with alkylaluminums, produce no butenes or only trace amounts of butenes.^{10,57} When using complex **2** as the pre-catalyst in the presence of 10 equivalents of methylaluminoxane (MAO), ethylene oligomerization was achieved at room temperature with a 0.09(1) s⁻¹ turnover frequency (TOF) for butenes (**Table 2**, entry 1) and 88(2)% selectivity for 1-butene (among the C₄ products), which is ~900 times faster than the reaction using complex **2** with AgBF₄ (**Table 1**, entry 3). However, the reaction products only contain ~12 wt. % of butenes (C₄), and a range of linear and 2-ethyl branched α -olefins were observed from C₆ to C₂₀ (**Scheme 4**).

The identity of the Al co-catalyst influences overall catalyst activity and selectivity. For example, changing the alkylaluminum co-catalyst from MAO to EtAlCl₂ results in a higher TOF (2.0(1) s⁻¹) with an increased mass fraction of C₄ olefins (~83 wt. %), while the reaction selectivity changes toward 2-butenes (**Table 2**, entry 2). By lowering the concentration of Ni pre-catalyst **2**, a faster TOF (13.2(3) s⁻¹) was observed with a slightly improved selectivity for 1-butene (**Table 2**, entry 3). Therefore, it is possible that the isomerization of 1-butene to 2-butene is a competing reaction with the ethylene dimerization/oligomerization process.

Different from using Ni pre-catalyst **2**, mixing pre-catalyst **3** with MAO gave an overall slower reaction with increased selectivity toward C₄ products (**Table 2**, entry 4). Using Et₂AlCl with **3** gave a slightly faster reaction (0.18(2) s⁻¹) while remaining selective for 1-butene (**Table 2**, entry 5), while the use of EtAlCl₂ with complex **3** significantly enhanced the TOF (2.5(3)s⁻¹) but changed the reaction selectivity towards 2-butenes (**Table 2**, entry 6). As shown in **Table 2** entries 7–10, lowering the concentration of **3** improves the 1-butene selectivity as well as providing an enhanced TOF until the Ni loading is decreased to 0.181 μmol. Similarly, when using MAO as the additive, decreasing the Ni loading from 9.05 to 0.905 μmol resulted in a higher TOF (**Table 2**, entry 4 vs 12). Lewis acidic AlCl₃ was also used as the co-catalyst with Ni pre-catalyst **3**, and gave ethylene dimerization to form 1-butene with a TOF = 0.139(4) s⁻¹ (**Table 2** entry 13). However, large amounts of Friedel–Crafts products from the reaction between toluene and ethylene/butenes were observed based on the GC-MS analysis. Therefore, due to the side reactions, the actual amount of C₄ products (*i.e.*, butenes) produced under this condition is low (8 wt. %) compared to the total consumption of ethylene. The Ni pre-catalyst (C^yPBP)NiBr (**4**) has also been tested with MAO as an additive (**Table 2**, entry 14), which proved to be selective for 1-butene, but also gave 1-hexene, 2-ethyl-1-butene and 3-methyl-1-pentene as side products (**Scheme 4**).

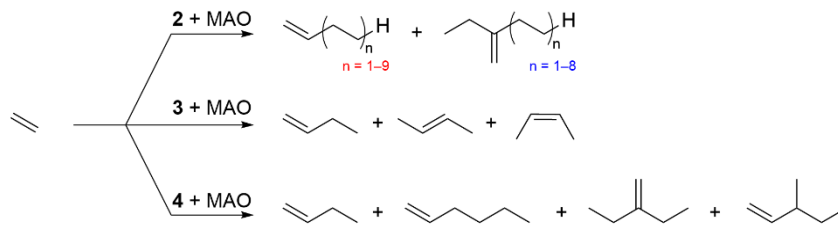
Table 2. Screening of aluminum co-catalyst and loading of Ni pre-catalyst on ethylene oligomerization.^a



Entry ^a	Ni complex	Loading (μmol)	Additive	TOF C ₄ ^b (s ⁻¹)	C ₄ wt%	α-C ₄ /C ₄ (%)	β-C ₄ /C ₄ (%)	
							<i>trans</i>	<i>cis</i>
1 ^c	2	9.05	MAO	0.09(1)	12	88(2)	4(1)	7(1)
2 ^c	2	9.05	EtAlCl ₂	2.0(1)	83	13.7(3)	55.6(4)	30.7(2)
3 ^c	2	0.905	EtAlCl ₂	13.2(3)	91	46(6)	32(4)	23(2)
4	3	9.05	MAO	0.037(3)	80	88(2)	6(1)	6(1)
5	3	9.05	Et ₂ AlCl	0.18(2)	95	79(2)	11(1)	10(1)
6	3	9.05	EtAlCl ₂	2.5(3)	90	16(1)	50(2)	35(2)
7	3	1.81	EtAlCl ₂	3.7(1)	92	29.6(8)	40.6(7)	29.8(4)
8	3	0.905	EtAlCl ₂	10.7(2)	94	29.5(1)	39.8(1)	30.7(2)
9	3	0.453	EtAlCl ₂	18.1(6)	92	35(3)	38(2)	28(1)
10	3	0.181	EtAlCl ₂	3(1)	92	83(2)	10(1)	8(1)
11	3	0.905	Et ₃ Al	0.20(2)	92	94(1)	3.7(5)	2.3(2)
12	3	0.905	MAO	0.18(1)	94	94.8(3)	3.0(1)	2.3(1)
13 ^d	3	0.905	AlCl ₃	0.139(4)	8	90(2)	7(1)	3(1)
14	4	0.905	MAO	2.7(2)	92	96.6(4)	2.0(3)	1.4(4)

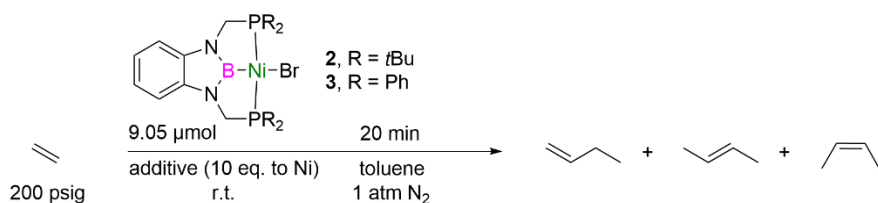
^a Reaction conditions: (R^RPBP)NiBr (9.05, 1.81, 0.905, 0.453, and 0.181 μmol); additive (10 equiv. relative to Ni pre-catalyst); using toluene as the solvent (1 mL total for each reaction); ethylene pressure was maintained at 200 psig using a Parr gas burette system. The total consumption of ethylene was measured based on the pressure change of the gas burette and used to calculate the weight percent of butenes in all reacted ethylene (C₄ wt. %). The reactions were performed at room temperature; however, the actual reaction temperature was unknown due to the exothermic nature of the reaction. Standard deviations were calculated from at least three independent experiments. ^b TOF C₄ = mol_{butenes} · mol_{Ni}⁻¹ · s⁻¹. ^c Longer chain products were detected. ^d Friedel–Crafts products from the reaction between toluene and ethylene/butenes were observed.

Scheme 4. Selectivity of ethylene oligomerization using (*t*BuPBP)NiBr (**2**), (PhPBP)NiBr (**3**) and (CyPBP)NiBr (**4**).



Effects of alkylating reagent and Lewis acid. To further understand the role of the alkylaluminum co-catalyst, different alkylating reagents were tested with the presence of Ni pre-catalyst **2** and **3**, as shown in **Table 3** entries 1–7. In all cases, no or only trace amounts of butenes (< 1 TO) were observed under the reaction conditions. Among these, the reaction of the Ni bromide complex **2** with Grignard reagent has been reported to form a stable (^tBuPBP)NiMe complex.⁵⁰ NaBH₄, a common hydride source used in the ethylene dimerization reaction,^{2,58} was also tested and gave no production of butenes upon combination with complex **3** (**Table 3**, entry 8). In addition, *in situ* NMR studies using (^tBuPBP)NiH with ethylene showed no activity in formation of butenes, instead, ethane was observed as the product and (^tBuPBP)NiH quickly decomposed to other species (**Figure S13**). This result is consistent with the previously reported olefin hydrogenation reactions using (^tBuPBP)NiH as the catalyst.⁴⁶ Therefore, we believe the ethylene dimerization and oligomerization reactions are not initiated by Ni–alkyl/hydride species such those proposed in the Cossee-Arlman type mechanism (see Introduction).

Since AlCl₃ with Ni pre-catalyst **3** was found to be active for the dimerization of ethylene, other Lewis acids such as BPh₃, BBr₃, and BF₃·OEt₂ were tested as an additive for the reaction (**Table 3**, entries 9–11). Among the results, BBr₃ with complex **3** showed activity for the production of 1-butene (TOF = 0.0013 s⁻¹), while using BF₃·OEt₂ as an additive gave a much faster ethylene dimerization with a TOF of 0.23(8) s⁻¹. The observation that Lewis acids without any hydride or alkyl sources (such as AlCl₃, BF₃, BBr₃) initiate the (^RPBP)Ni catalyzed ethylene dimerization is consistent with our proposal that the catalytic ethylene oligomerization reaction is not likely initiated by a Ni–alkyl/hydride species.

Table 3. Alkylating reagents and Lewis acids.^a

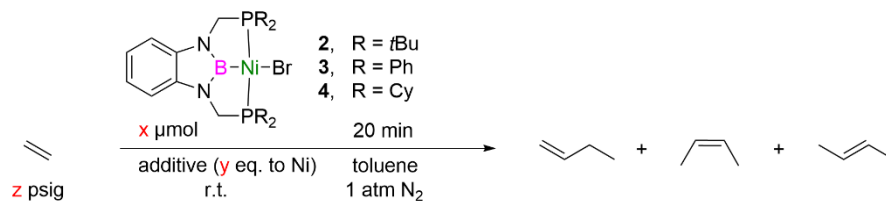
Entry ^a	Ni complex	Additive	TOF C ₄ ^b (s ⁻¹)	C ₄ /C _n (%)	α-C ₄ /C ₄ (%)	β-C ₄ /C ₄ (%)	
						<i>trans</i>	<i>cis</i>
1	2	EtMgBr	N.D.	–	N.D.	N.D.	N.D.
2	2	MeMgBr	N.D.	–	N.D.	N.D.	N.D.
3	2	MeLi	N.D.	–	N.D.	N.D.	N.D.
4	2	Me ₂ Mg	N.D.	–	N.D.	N.D.	N.D.
5 ^c	3	EtMgBr	trace	–	trace	trace	trace
6	3	MeLi	N.D.	–	N.D.	N.D.	N.D.
7	3	Me ₂ Mg	N.D.	–	N.D.	N.D.	N.D.
8	3	NaBH ₄	N.D.	–	N.D.	N.D.	N.D.
9 ^{c,d}	3	BPh ₃	trace	–	trace	trace	trace
10 ^d	3	BBr ₃	0.0013	> 99	86	10	4
11 ^d	3	BF ₃ ·OEt	0.23(8)	95(1)	79.8(5)	10.4(5)	9.7(1)

^a Reaction conditions: (^RPBP)NiBr (9.05 μmol); additive (10 equiv. to Ni pre-catalyst); using toluene as the solvent (1 mL total for each reaction); ethylene pressure was maintained at 200 psig using the Parr gas burette system. The reactions were performed at room temperature; however, the actual reaction temperature was unknown due to the exothermic nature of the reaction. The mol% of butenes in all observed olefins (C₄/C_n) was determined by GC-MS. Standard deviations were calculated from at least three independent experiments. ^b TOF C₄ = mol_{butenes} · mol_{Ni}⁻¹ · s⁻¹ ^c The observed amounts of products were less than 1 TO. ^d Using 0.905 μmol of Ni pre-catalyst.

Optimization of reaction parameters. Different reaction parameters such as Al/Ni ratio, Ni pre-catalyst loading, and ethylene pressure were optimized using complexes **2**, **3**, and **4** with MAO or EtAlCl₂ as shown in **Table 4**. We found that in general the TOF of butenes increases with the Al/Ni ratio (**Table 4**, entry 1 vs 2, 3 vs 4, 6 vs 7, 10 vs 11, 13 vs 14, 15 vs 16, 18 vs 19, 20 vs 21, 24 vs 25) as well as the dilution of the Ni pre-catalyst loading (**Table 4**, entry 2 vs 3, 7 vs 9, 14 vs 15, 19 vs 20 vs 24). The reaction is exothermic, as the temperature rises upon addition of ethylene gas. Therefore, a set of experiments was performed with external cooling of the VCO steel reactor using an ice bath, which resulted in a slightly faster rate and better selectivity for 1-butene

compared to the reaction at room temperature without cooling (**Table 4**, entry 7 vs 8). This suggests that higher reaction temperatures might not be beneficial for the reaction and, instead, could potentially lead to faster isomerization of 1-butene to 2-butenes, as well as possible decomposition of the active Ni species. Decreasing the loading of Ni pre-catalyst also generates less heat during the reaction, which could partially rationalize the increase in TOF when diluting the Ni pre-catalyst. When using EtAlCl₂ as the co-catalyst, increasing the ethylene pressure resulted in better selectivity for 1-butene (**Table 4**, entry 11 vs 12, 23 vs 24, 25 vs 26), while using MAO gave an opposite trend (**Table 4**, entry 4 vs 5, 16 vs 17). The difference in selectivity based on ethylene pressure is potentially rationalized by competition between ethylene dimerization, 1-butene to 2-butenes isomerization, and dimerization/oligomerization of butene upon reaction with ethylene. Using the more C₄ selective co-catalyst (*i.e.*, EtAlCl₂), higher ethylene pressure suppresses 1-butene isomerization, while with the less C₄ selective co-catalyst (*i.e.*, MAO), higher ethylene pressure favors the potential dimerization/oligomerization of butene with ethylene that might consume 1-butene and 2-butene at different rates with 1-butene being converted to higher olefins more rapidly than 2-butenes, thus decreasing the 1-butene to 2-butenes ratio. For all tested conditions, complex **2** with 1000 equivalents of EtAlCl₂ under 600 psig of ethylene, gave the fastest reaction which was selective for 1-butene with a TOF of 33(2) s⁻¹ and 87.2(3)% selectivity (**Table 4**, entry 12). Whereas, complex **3** under the same conditions achieved the best overall TOF of butenes (274(34) s⁻¹), but only 41(1)% selectivity for 1-butene (**Table 4**, entry 26).

Table 4. Effect of different reaction parameters on ethylene dimerization with (^RPBP)NiBr with alkylaluminum.^a



Entry ^a	[Ni]	Loading (μmol)	C ₂ H ₄ (psig)	[Al]	Al/Ni ratio	TOF C ₄ (s ⁻¹)	α-C ₄ /C ₄ (%)	C ₄ /C _n (%)	TOF C ₆ (s ⁻¹)
1 ^c	2	9.05	200	MAO	1	0.0012(1)	64(3)	20(2)	0.0004(1)
2 ^c	2	9.05	200	MAO	10	0.09(1)	88(2)	9(1)	0.10(1)
3 ^c	2	0.905	200	MAO	10	0.52(1)	97.5(2)	20.8(4)	0.27(1)
4 ^c	2	0.905	200	MAO	1000	2.2(2)	92.6(1)	6(1)	3.0(5)
5 ^c	2	0.905	600	MAO	1000	9(2)	80(1)	7.3(4)	10(3)
6 ^c	2	9.05	200	EtAlCl ₂	1	0.023(2)	94(1)	28(2)	0.0079(3)
7 ^c	2	9.05	200	EtAlCl ₂	10	2.0(1)	13.7(3)	86(1)	0.29(2)
8 ^{c,d}	2	9.05	200	EtAlCl ₂	10	2.8(5)	21.0(3)	85(2)	0.36(1)
9 ^c	2	0.905	200	EtAlCl ₂	10	13.2(3)	46(6)	89(1)	0.97(6)
10 ^c	2	0.453	200	EtAlCl ₂	10	1.3(2)	89(1)	47(2)	0.30(5)
11 ^{c,e}	2	0.453	200	EtAlCl ₂	1000	45(1)	47.6(3)	92.4(3)	2.1(1)
12 ^{c,e}	2	0.453	600	EtAlCl ₂	1000	33(2)	87.2(3)	94.2(1)	0.8(1)
13	3	9.05	200	MAO	1	0.0033(2)	92.9(2)	–	N.D.
14	3	9.05	200	MAO	10	0.037(3)	88(2)	>98	0.0003
15	3	0.905	200	MAO	10	0.18(1)	94.8(3)	95.7(1)	0.0026(2)
16	3	0.905	200	MAO	1000	34(3)	15.5(3)	89(1)	3.7(2)
17	3	0.905	600	MAO	1000	66(4)	11.4(3)	69(2)	23(1)
18	3	9.05	200	EtAlCl ₂	1	0.24(5)	69(10)	95.7(3)	0.010(2)
19	3	9.05	200	EtAlCl ₂	10	2.5(3)	16(1)	81(1)	0.46(8)
20	3	0.905	200	EtAlCl ₂	10	10.7(2)	29.5(1)	89.5(3)	1.1(1)
21	3	0.905	200	EtAlCl ₂	100	27(5)	20(1)	84(2)	4.2(6)
22 ^e	3	0.905	600	EtAlCl ₂	1000	110(13)	22(1)	85(2)	15(4)
23	3	0.453	100	EtAlCl ₂	10	5.4(1)	22(1)	85(1)	0.81(4)
24	3	0.453	200	EtAlCl ₂	10	18.1(6)	35(3)	92(1)	1.3(1)
25 ^e	3	0.453	200	EtAlCl ₂	1000	115(17)	18(1)	91(1)	9(2)
26 ^e	3	0.453	600	EtAlCl ₂	1000	274(34)	41(1)	88(3)	30(3)
27	4	0.905	200	MAO	10	2.7(2)	96.6(4)	90(1)	0.29(5)
28	4	0.905	200	MAO	1000	22(1)	33.1(1)	41(3)	19(2)
29	4	0.905	200	EtAlCl ₂	10	14(1)	60(4)	83(2)	2.5(5)
30	4	0.905	200	EtAlCl ₂	1000	20(2)	40(3)	94.2(3)	0.9(1)

^a Reaction conditions: (^RPBP)NiBr (9.05, 0.905 and 0.453 μmol); additive (1, 10, 100 and 1000 equiv. to Ni pre-catalyst); using toluene as the solvent (1 mL total for each reaction); ethylene pressure was maintained at 100, 200 or 600 psig using the Parr gas burette system. The reactions are performed at room temperature; however, the actual reaction temperature is unknown due to the exothermic nature of the reaction. The mol% of 1-butene in butenes (α-C₄/C₄), and butenes in all observed olefins (C₄/C_n) were determined by GC-MS. N.D. = not detected. Standard deviations are calculated from at least three independent experiments. ^b TOF C₄ = mol_{butenes} · mol_{Ni}⁻¹ · s⁻¹ ^c Longer chain products were detected. ^d The VCO reactor was cooled with an ice bath during the reaction. ^e Reaction was monitored after 10 min.

Comparison of previously reported Ni catalysts. **Table 5** compares selected results of our newly reported catalysis with previously reported homogeneous Ni catalysts which demonstrated activity for ethylene dimerization.^{2,4,55-56,59-65} Although a direct comparison of previously reported catalysts is not possible since the reactions were performed under different conditions (*e.g.*, pressure, temperature, Ni catalyst concentration, Al/Ni ratio, etc.), the comparative data provide some reasonable comparison points. The activities given in **Table 5** were all converted into a commonly used unit $\text{g}_{\text{oligomers}} \cdot \text{mol}_{\text{Ni}}^{-1} \cdot \text{h}^{-1}$ for each catalytic system. The overall TOFs given in **Table 5** were calculated based on ethylene consumption, for which $\text{TOF} = \text{activity}/(\text{molar mass of } \text{C}_2\text{H}_4)$ with a unit of $\text{mol}_{\text{ethylene}} \cdot \text{mol}_{\text{Ni}}^{-1} \cdot \text{s}^{-1}$. In general, most of the reported highly active Ni catalysts are supported by SHOP-type and related phosphine-sulfur-, phosphine-, nitrogen-based ligand structures. In addition to the ethylene polymerization reaction reported by the Nozaki group,⁵¹ there are only a limited number of ligand structures with a central boron center.⁶⁶ As outlined in **Table 5**, the new ^RPBP ligated Ni complexes reported in this work exhibit relatively high activities for the ethylene dimerization reaction, which motivated us to better understand the reaction pathway (see below).

Table 5. Comparison of previously reported homogeneous Ni catalysts for ethylene dimerization to our newly reported PBP-Ni catalysis.^a

Ligand type	co-catalyst	Activity ^a g/(mol _{Ni} ·h)	TOF _{ethylene} ^b (s ⁻¹)	α-C ₄ /C ₄ (%)	C ₄ /C _n (%)	Temp. (°C)	ref
(P,P)	EtAlCl ₂	2.4 × 10 ⁸	2377	35	82	45	(55)
(O,N,S)	MAO	1.4 × 10 ⁸	1411	16	90	0	(56)
(N,N)	Et ₃ Al ₂ Cl ₃	4.6 × 10 ⁷	460	92	88	r.t.	(59)
(N,N,N)	Et ₂ AlCl/PPh ₃	4.0 × 10 ⁷	391	12	92	20	(60)
(N,N)	MAO	1.9 × 10 ⁷	190	56	90	35	(61)
(P,O)	None	1.9 × 10 ⁷	183	99	85	40	(67)
(N,N,O)	MAO	1.2 × 10 ⁷	119	18	83	45	(62)
(P,N)	EtAlCl ₂	9.1 × 10 ⁶	90	23	98	40	(63)
(N,O)	Et ₂ AlCl	6.6 × 10 ⁶	65	100	100	30	(64)
(N,N)	Et ₂ AlCl	4.7 × 10 ⁶	46	> 99	77	45	(65)

(^t BuP,B,P)	EtAlCl ₂	6.9 × 10 ⁶	68	87	94	r.t.	<i>this</i>
(^{Ph} P,B,P)	EtAlCl ₂	6.5 × 10 ⁷	640	41	89	r.t.	<i>work</i>

^a Most of the catalysts activities in this table were originally reported in g_{oligomers}·mol_{Ni}⁻¹·h⁻¹, thus we converted all data to the same units for comparison. ^b Based on ethylene consumption, for which TOF = activity/(28.05 g/mol) with the unit of mol_{ethylene}·mol_{Ni}⁻¹·s⁻¹.

Isomerization of 1-butene. As noted above, we speculate that the isomerization process for the conversion of 1-butene to 2-butenes could be a separate competing reaction in the catalytic ethylene dimerization/oligomerization using Ni pre-catalysts **2** or **3**. Therefore, a set of experiments using 1-butene as the only substrate with EtAlCl₂ or MAO as the co-catalyst with and without Ni pre-catalyst **2** or **3** were performed (**Figure 1**). Similar to the reaction using propylene as a substrate, no dimerization or oligomerization products of butenes were found based on the GC-MS analysis. While both complex **2** and **3** were able to isomerize 1-butene to 2-butenes in the presence of EtAlCl₂ or MAO, control experiments using only EtAlCl₂ or MAO showed much slower rates of isomerization of 1-butene to 2-butenes. Using the Ni pre-catalyst **3** approximately 10-fold faster isomerization of 1-butene to 2-butenes was observed compared to pre-catalyst **2** under the conditions using EtAlCl₂, which is consistent with the observed ligand effect on 1- vs 2-butene selectivity of the ethylene dimerization reactions (see **Table 1**, and **Table 4**, entry 6 vs 18, 9 vs 21, 10 vs 24, 11 vs 25, 12 vs 26). As noted above, this ligand effect (*i.e.*, 2-butenes vs. 1-butene selectivity as a function of identity of PBP ligand) can be rationalized by the presence of a more sterically hindered ^tBu group in complex **2** inhibiting 1-butene coordination, and thus retarding the rate of 1-butene isomerization. In addition, using EtAlCl₂ with and without Ni pre-catalyst gave a much faster isomerization compared to MAO, which is also consistent with the observed difference in 1- vs 2-butene selectivity when using EtAlCl₂ or MAO as additive (see **Table 4**, entries 2 vs 7, 3 vs 9, 13 vs 18, 14 vs 19, 15 vs 20). Although the experimental evidence

cannot completely rule out the possibility of direct reaction pathways from ethylene to 2-butenes, it seems reasonable to conclude that 2-butenes can be produced via a Ni catalyzed isomerization process of 1-butene, which is a competing reaction during the catalytic ethylene dimerization/oligomerization reaction.

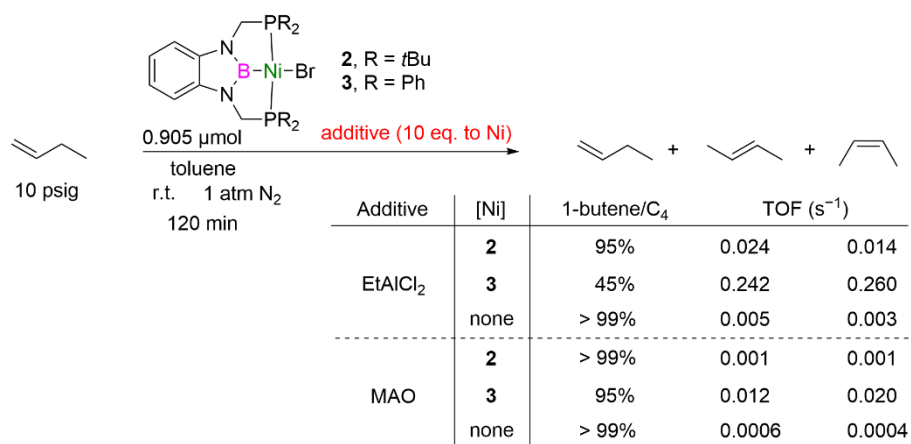


Figure 1. Isomerization of 1-butene. Reaction conditions: (^RPBP)NiBr (0.905 μmol); EtAlCl₂ (9.05 μmol); using toluene as the solvent (1 mL total for each reaction); 10 psig 1-butene at room temperature for 120 min.

***In situ* NMR experiments and kinetic studies.** To gain better understanding of the reaction mechanism using Al co-catalyst, experiments have been conducted using (^RPBP)NiBr complex **2** and **3** with the presence of EtAlCl₂. The *in situ* NMR studies only showed line broadening after addition of EtAlCl₂ (see Supporting information, Sections 4.6–4.8), which could be due to a fluxional process between (^RPBP)Ni(Br–LA) and (^RPBP)Ni(Cl–LA) that is assisted by the Lewis acidic aluminum salt (LA). Using complex **2** with EtAlCl₂, a crystal of (^tBuPBP)Ni(AIX₄) (X = Br or Cl, **5-AIX₄**) was isolated and studied by single crystal X-ray diffraction (**Figure 2** and **Figure S45**), in which Br is partially occupying some of the Cl sites to make a mixed halide AIX₄ anion. This observation further supports our proposed fluxional process. In addition, the Ni–Cl bond

distances in the solid state structures are in the range of 2.378(18) to 2.413(9) Å, longer than that in the (*t*BuPBP)NiCl complex {2.2399(4) Å}.⁴⁶ In addition, this fluxional process has also been supported by DFT calculations (**Figure S53**), where the (*t*BuPBP)Ni(X–AlCl₃) complex seems to be lowest-energy species of the process.

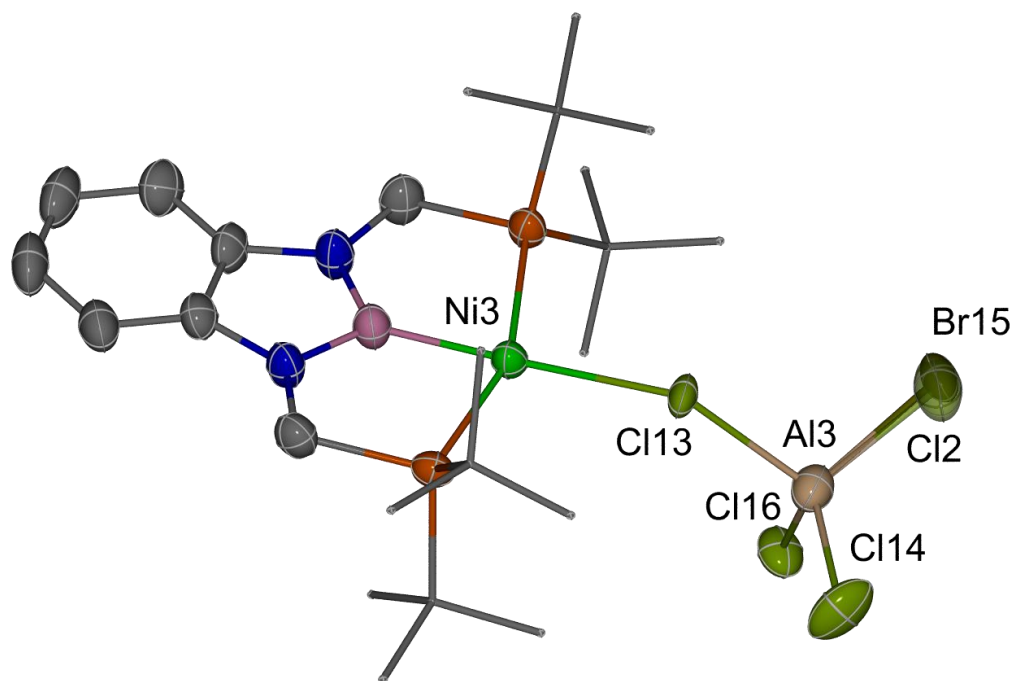


Figure 2. ORTEP of (*t*BuPBP)Ni(AlX₄) (X = Br or Cl, **5-AlX₄**). Ellipsoids are drawn at 50% probability level. The *t*Bu groups were set to stick mode for clarity. Some of the hydrogen atoms, solvent molecules and the other repeated molecules in the unit cell have been removed for clarity. Selected bond lengths (Å): Ni3–Cl13 2.4013(10), Al3–Cl13 2.2303(16), Al3–Cl14 2.1376(18), Al3–Cl2 2.126(9), Al3–Cl16 2.1741(19).

The TOFs of ethylene dimerization reactions using complex **3** with EtAlCl₂ under variant constant ethylene pressures were monitored (**Table S4**). As it shown in **Figure 3**, at low ethylene pressures, a second-order dependence of rate on [C₂H₄] was observed; while at high ethylene pressures, apparent saturation kinetics and a transition toward a first-order dependence was observed. The saturation kinetics can be rationalized by the proposed reversible coordination of

ethylene, which could lead to saturation kinetics at higher $[C_2H_4]$ (**Figure 4**). These results are consistent with our proposed mechanism based on DFT calculations (see below).

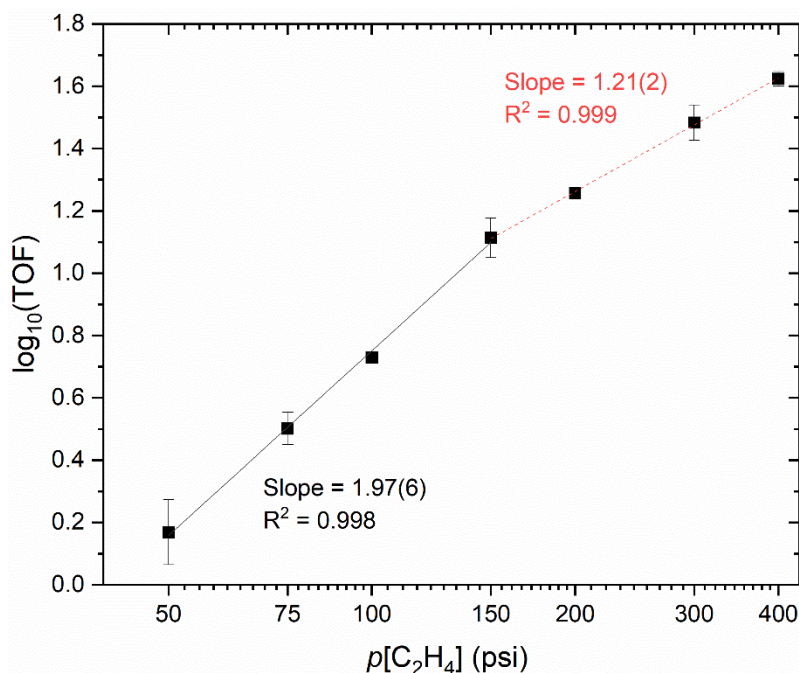


Figure 3. Log-log plot of TOF versus ethylene pressure.

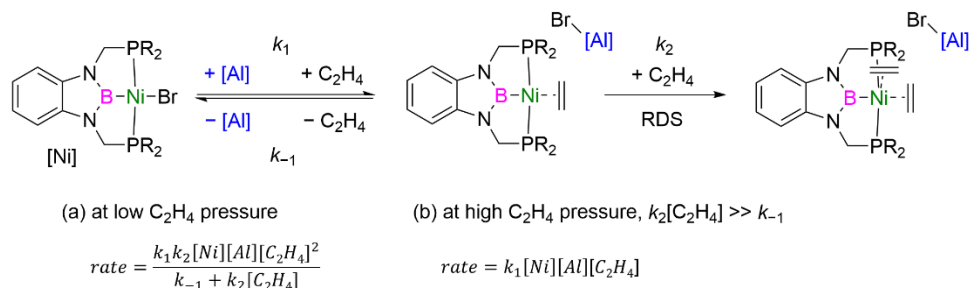
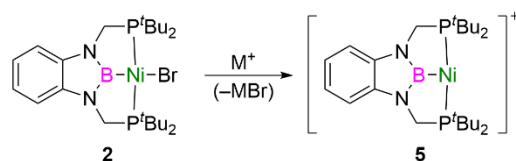


Figure 4. Simplified potential rate law of the reaction using $(R^PBP)NiBr$ with Al co-catalyst.

DFT analysis on the reaction mechanism. The aforementioned experimental data point to a mechanism for which the $[(R^PBP)Ni]^+$ fragment plays a fundamental role in the dimerization of ethylene to yield 1-butene. Indeed, control experiments revealed the participation of both the PBP ligand and nickel in the process, and stoichiometric experiments ruled out the likely involvement

of nickel acetate, hydride, or alkyl species. Therefore, we conducted DFT studies using cationic complex **5** (**Scheme 5**), produced from the reaction between bromide species **2** and a halide abstractor (*e.g.*, AgBF₄, NaBAr^F, AgBAr^F, etc.). Calculations were carried out at the PBE0/def2TZVP/def2QZVP level of theory, including Grimme's D3 dispersion correction (PBE0-D3, see SI for information and references), using **5** and ethylene as the energy reference.

Scheme 5. Simplified pathway for halide abstraction from complex **2** to give cationic complex **5**.



Coordination of one ethylene molecule to the vacant position of [(^tBuPBP)Ni]⁺ (**5**) to give [(^tBuPBP)Ni(η²-C₂H₄)]⁺ (**5**·C₂H₄) is isoenergetic (−0.02 kcal mol^{−1}) to the reactants. From this point, several mechanistic scenarios were considered, most of which afforded kinetic barriers too energy-demanding to overcome experimentally (energy profiles for the energetically inaccessible pathways can be found in the Supporting Information). Activation of a C–H bond of bound ethylene (ΔG[‡] > 50 kcal mol^{−1}) of **5**·C₂H₄ gave Ni–vinyl and B–H fragments in a less thermodynamically stable geometry than the initial cationic Ni–ethylene π complex (23.4 kcal mol^{−1} difference, **Figure S47**). Including weakly coordinating anions such as BF₄[−] in the calculations led to even higher Gibbs free energy values (**Figure S52**). The addition of a free ethylene molecule to the coordinated ethylene of **5**·C₂H₄ was also computed, based on the study by Bernardi, Bottoni *et al.*²¹ This resulted in the desired **5**·1-butene complex (−18.1 kcal mol^{−1}), yet at the expense of very high energy transition states (**Figure S48**).⁶⁸ Exploratory calculations

involving [2+2] cycloaddition pathways did not lead to chemically meaningful results. Finally, dissociation of one of the phosphine ligands (**Figure S49**) or coordination of the ethylene molecule across the Ni–B bond (**Figure S51**) gave energy barriers above 30 kcal mol⁻¹ along with thermodynamically unstable products. However, coordination of a second ethylene molecule to **5**·C₂H₄ opened the door to a new ethylene dimerization mechanism involving participation of the PBP ligand.

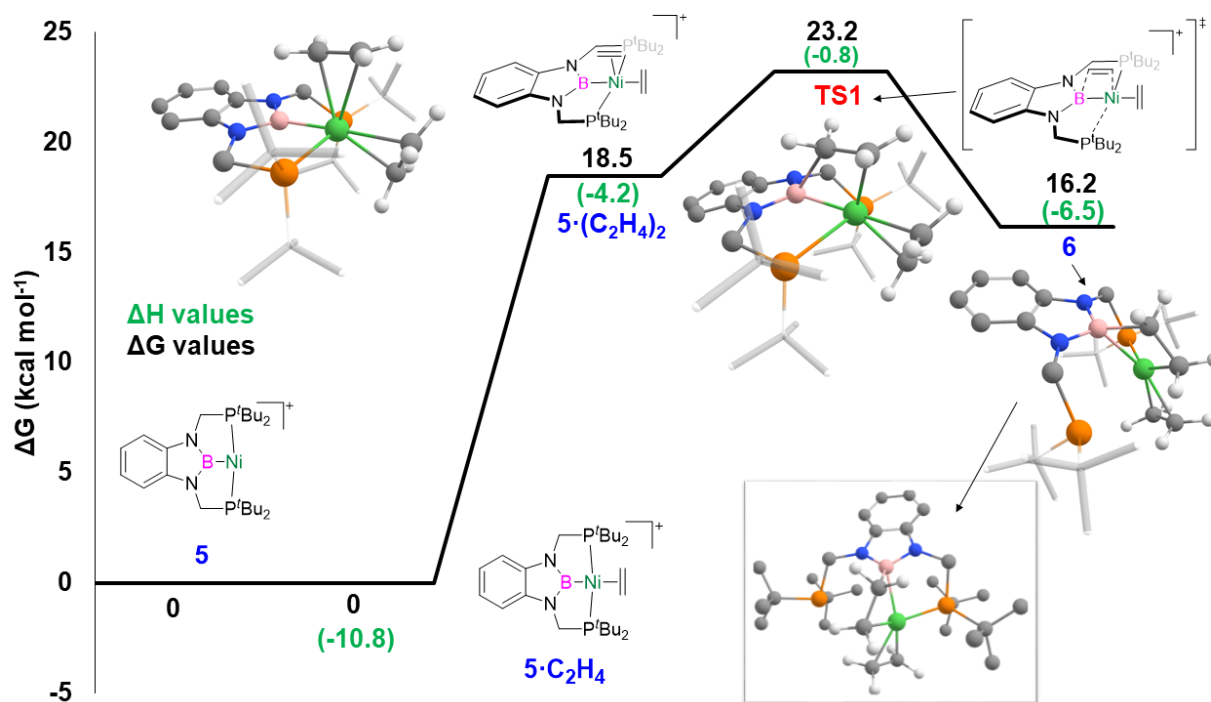


Figure 5. Excerpt of the Gibbs energy profile for the reaction of two equivalents of ethylene and [(^tBu)PBP]Ni⁺ (**5**) to form a product **6** with two ethylene ligands and a dissociated phosphine. Relative Gibbs energies at 298 K and 1 M in kcal mol⁻¹. Hydrogen atoms on the (^RPBP)Ni moiety have been omitted for clarity. Enthalpy values highlighted in green.

Figure 5 shows a calculated pathway for (^RPBP)Ni-mediated positioning of two ethylene molecules for subsequent C–C coupling. Ethylene binding to give complex **5**·(C₂H₄)₂ is thermodynamically unfavorable (18.5 kcal mol⁻¹ higher than **5**·C₂H₄), as depicted in **Figure 5**.

This is in line with our previous studies on H₂ activation by neutral, square planar Ni(II) complexes,^{50,69} for which the filled d_{z²} orbital on nickel gave rise to weak σ-H₂ complexes.⁷⁰ Indeed, **5**·(C₂H₄)₂ exhibits very little C=C bond elongation upon binding (1.36 Å vs 1.33 Å in free ethylene). Nonetheless, molecular orbital analysis of ethylene and **5**·C₂H₄ (**Figure 6**) point to potential orbital overlap involving the PBP ligand {HOMO (**5**·C₂H₄) → LUMO (ethylene)} that can lead to ethylene functionalization. In fact, this second ethylene molecule binds across the Ni–B bond in transition state **TS1** (23.2 kcal mol⁻¹) to form a 4-membered borametallacycle, simultaneously promoting dissociation of one of the phosphine ligands from the metal center, as observed in the product **6** (**Figure 5**).

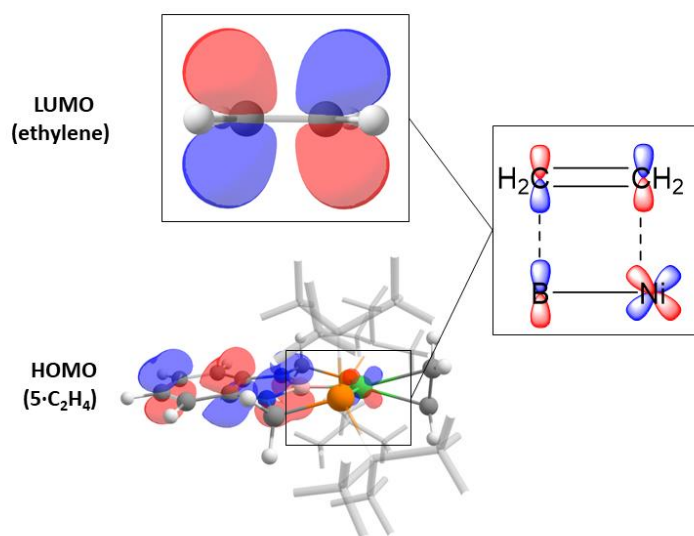


Figure 6. Frontier molecular orbitals involved in **TS1**, which provides C–C formation between two equivalents of ethylene.

Complex **5** is 16.2 kcal mol⁻¹ above the reactants, which suggests the formation of **5** is possibly reversible. However, the rest of the kinetic barriers are lower than **TS1**, and the high thermodynamic stability of the product makes the overall process energetically downhill and favorable towards the formation of the experimentally observed 1-butene (see below). The

calculated phosphine dissociation is probably due to steric clash between the ethylene moieties and the *tert*-butyl substituents on the phosphorus atom. In fact, both ethylene ligands in **6** are oriented towards the space previously occupied by the phosphine ligand (**Figure 5**, inset). The short C...C distance (2.37 Å) observed for the two closer carbon atoms suggests preorganization of both ethylene fragments for subsequent C–C coupling. The C–C bond formation between two ethylene ligands is calculated to proceed through **TS2** (17.1 kcal mol⁻¹), located only 0.9 kcal mol⁻¹ higher than complex **6** (**Figure 7**). The next intermediate after **TS2** (species **7**, 13.9 kcal mol⁻¹) contains a six-membered B–C_δ–C_γ–C_β–C_α–Ni ring, with C–C distances ranging from 1.50 to 1.67 Å. Although the distance arrangement might suggest some butadiene character, these C–C bonds are longer than those observed in 1,3-butadiene (1.34–1.45 Å).⁷¹ From complex **7**, numerous hydrogen atom migrations have been explored to form either B–H or new C–H bonds, giving too energy demanding ($\Delta G^\ddagger > 30$ kcal mol⁻¹) kinetic barriers. However, the C_β atom can orient one of its hydrogen atoms closer to the metal center with minimal energy cost (**TS3** = 12.8 kcal mol⁻¹), in order to achieve a suitable structure for a β-hydride elimination step. The outcome of this rearrangement is complex **8**, which exhibits an agostic interaction⁷² through the C_β–H bond (Ni–H = 1.78 Å, Ni–C = 2.11 Å, Ni–H–C = 89.2°), located trans to the bound phosphine ligand. Although this complex is rather low in Gibbs free energy (7.9 kcal mol⁻¹), we found a different, more energy-demanding isomer (**8'**, 19.7 kcal mol⁻¹) where the C_β–H bond and the bound phosphine are in a *cis* orientation, and the 3c-2e interaction exhibits a much shorter Ni–H bond (1.55 Å), with similar Ni–C (2.11 Å) and Ni–H–C (96.9°) metrics to those observed for **7**. Complex **8'** proceeds to a β-H elimination transition state (**TS4**) with a free energy of activation of only 0.3 kcal/mol.

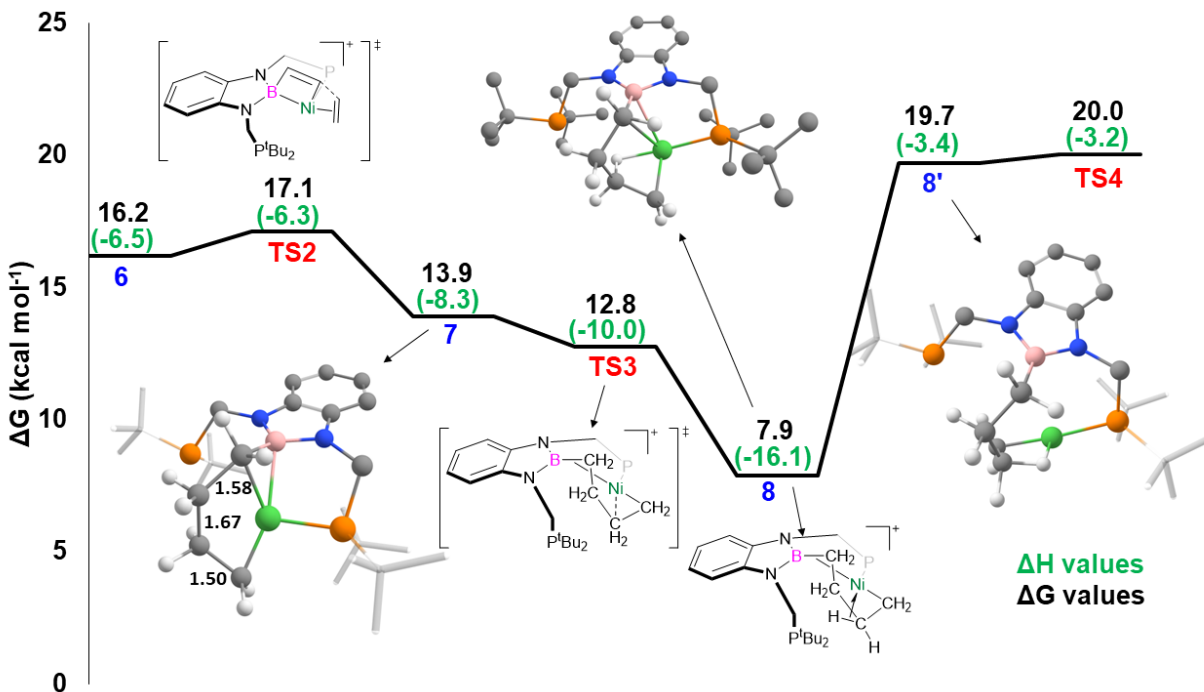


Figure 7. Excerpt of the Gibbs energy profile for Ni-mediated C–C coupling of two ethylene ligands (**TS2**) to ultimately form complex **8**, which possesses a Ni/CH agostic interaction. Relative Gibbs energies at 298 K and 1 M in kcal mol⁻¹. Hydrogen atoms on the (^RPBP)Ni system have been omitted for clarity. Enthalpy values highlighted in green.

The geometry of **8'** is very similar to that observed for **TS4** (early transition state), which might explain why the first β -hydride elimination step is only 0.3 kcal mol⁻¹ higher in energy (**Figure 8**). After **TS4**, intermediate **9** (12.4 kcal mol⁻¹) contains the newly formed C=C double bond (C=C distance = 1.36 Å) bound to nickel, along with coordination of one of the phosphines and the new hydride ligand. In addition, the fourth Ni-coordination position is stabilized by a weak σ interaction with the B–C δ bond (B–Ni = 2.76 Å C–Ni = 2.48 Å). Although one might think that 1-butene is practically formed, exploratory calculations involving hydride transfer to C δ or B to release the experimentally observed product led to high (> 30 kcal mol⁻¹) energy barriers. Nevertheless, **TS5** (11.6 kcal mol⁻¹) was found, which reveals the stretch of the B–C \rightarrow Ni interaction along its imaginary frequency, giving rise to species **10** (10.8 kcal mol⁻¹). In this geometry, an agostic

interaction through the C_δ-H bond is observed (Ni-H = 1.88 Å, Ni-C = 2.28 Å, Ni-H-C = 95.5°) along with shorter Ni···C distances (ranging from 0.05 to 0.2 Å) for all the carbon atoms coming from the ethylene fragments. Next, hydride transfer to C_α occurs via **TS6**, located 15.6 kcal mol⁻¹ above the energy reference. This hydride transfer process leads to intermediate **11** (14.8 kcal mol⁻¹), which contains a new nickel-carbon bond (Ni-C_β = 1.89 Å) and two agostic interactions: the previous one observed for the C_δ-H bond, and another for one of the C_α-H bonds of the new CH₃ group. In a similar fashion to intermediates **8** and **8'**, isomer **11'** was found, where both agostic interactions are replaced by two different ones: one C-H bond from one of the *tert*-butyl groups of the bound phosphine, and a C-H bond from C_γ. This bonding arrangement is again suitable for a β-hydride elimination step, which indeed proceeds through **TS7**, located only 0.6 kcal mol⁻¹ above **11'**. This event leads to the formation of an internal double bond in the tetracarbon chain of complex **12** (10.4 kcal mol⁻¹). From this point, it seems reasonable that the hydride ligand can be transferred to C_δ to rationalize the formation of *trans* 2-butene. However, relaxed potential energy scan calculations revealed hydride transfer to C_γ instead (*i.e.*, formation of intermediate **11**), probably due to its closer proximity and the relative stability of such geometry.

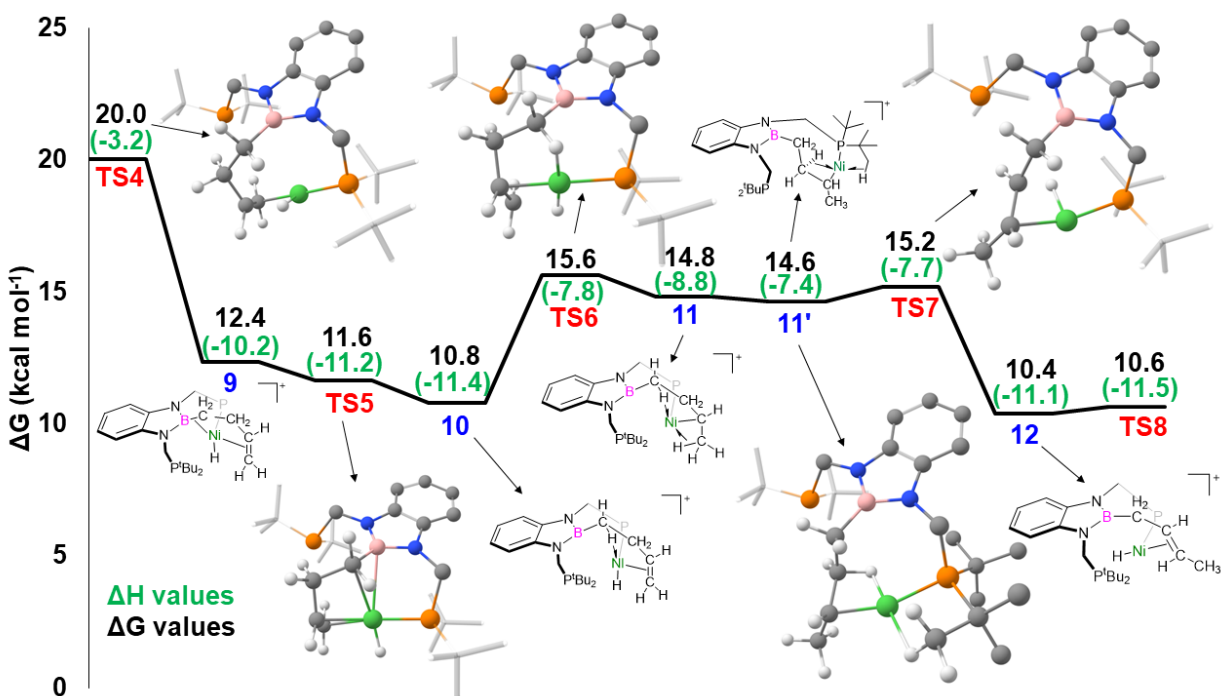


Figure 8. Excerpt of the Gibbs energy profile for the reaction of ethylene and **5** (β -hydride eliminations and hydride transfer). Relative Gibbs energies at 298 K and 1 M in kcal mol⁻¹. Hydrogen atoms on the (^RPBP)Ni system have been omitted for clarity. Enthalpy values highlighted in green.

Complex **12** features a nickel center with a T-shaped geometry for which the hydride ligand is pointing to the boryl fragment. Therefore, it needs to orbit around the metal in order to give 1-butene. This orbiting movement requires negligible energy (**TS8**, 10.6 kcal mol⁻¹) and places the hydride ligand close to C β (H \cdots C β = 2.53 Å, intermediate **13**, **Figure 9**) for subsequent transfer, which takes place via **TS9** (14.6 kcal mol⁻¹). Interestingly, this transition state also involves the formation of the C δ =C γ double bond and the cleavage of the B–C δ bond, giving species **14**. In this intermediate, the nickel atom adopts a distorted square planar geometry in which 1-butene is bound to nickel through the double bond and one agostic interaction. Thus, phosphine coordination can easily occur (**TS10**, 6.6 kcal mol⁻¹), displacing the C–H bond and regenerating the pincer scaffold in **5**·1-butene (–18.1 kcal mol⁻¹). Finally, regeneration of cationic complex **5** and dissociation of the 1-butene is the most stable step in the entire process, as expected (–19.3 kcal mol⁻¹).

This proposed mechanism highlights the crucial role of the PBP ligand in the catalytic dimerization of ethylene. First, its tridentate nature allows the approach of one equivalent of ethylene to the vacant position of a square planar, cationic Ni(II) complex. Then, the boryl fragment facilitates coordination of a second ethylene molecule, and serves as an anchoring point for one of the ends of the tetracarbon chain, allowing hydrogen atom rearrangement throughout the entire cycle while keeping the substrate bound to the catalyst. Lastly, the hemilabile character of the phosphine groups on the pincer scaffold is instrumental for the development of the elementary steps in the cycle, since they can dissociate when needed to create a vacant position in the coordination sphere, which they can also stabilize by means of agostic interactions through the substituents on phosphorus.

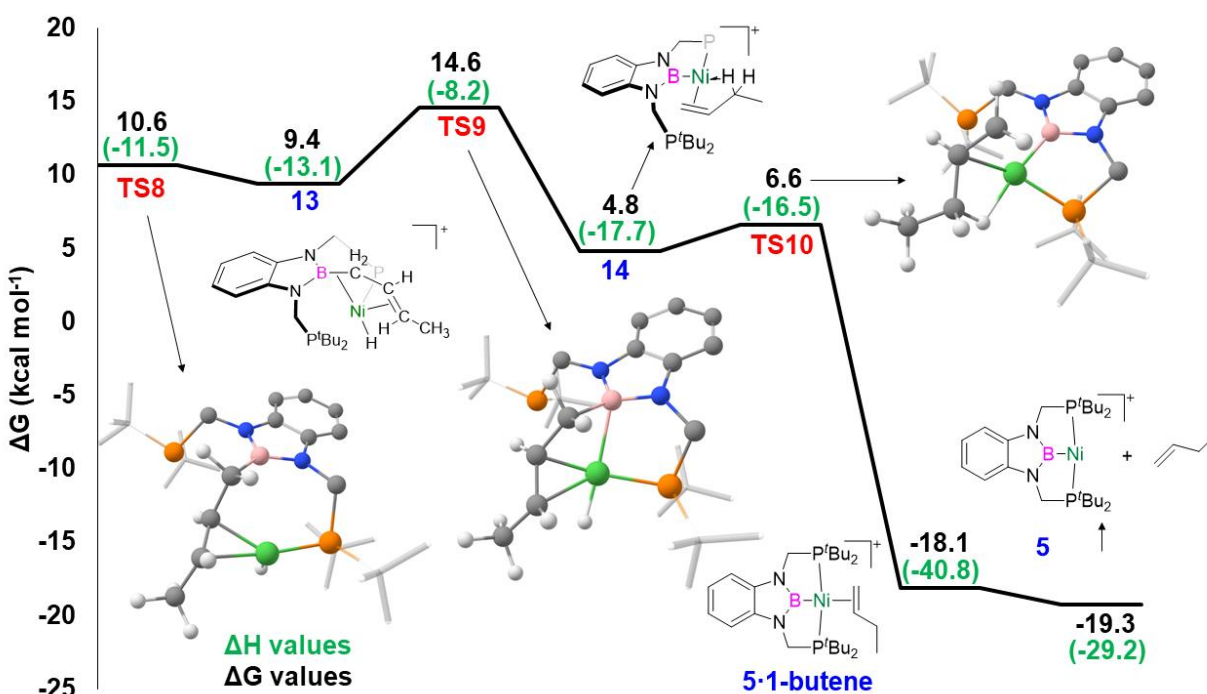


Figure 9. Excerpt of the Gibbs energy profile for the reaction of ethylene and **5** (hydride) and formation of 1-butene). Relative Gibbs energies at 298 K and 1 M in kcal mol⁻¹. Hydrogen atoms on the (^RPBP)Ni system have been omitted for clarity. Enthalpy values highlighted in green.

Summary and Conclusions

We have demonstrated that ^RPBP-Ni complexes are active catalysts for ethylene dimerization/oligomerization. Our studies revealed that the ethylene dimerization is generally selective for the formation of terminal 1-butene, and that the features of catalysis are dependent on ligand identity. The reactions proceed by using (^tBuPBP)NiOAc (**1**) without co-catalyst, as well as mixing (^RPBP)NiBr (**2** or **3**) with Ag⁺ or Na⁺ salts, alkylaluminum, or other Lewis acids (*e.g.*, BF₃, BBr₃, and AlCl₃). The (^{Ph}PBP)Ni complex **3** shows significant activity for the production of butenes with a TOF up to 274(34) mol_{butenes}·mol_{Ni}⁻¹·s⁻¹ (41(1)% selective for 1-butene), while the (^tBuPBP)Ni complex **2** shows good selectivity for 1-butene with a TOF up to 33(2) mol_{butenes}·mol_{Ni}⁻¹·s⁻¹ (87.2(3)% selective for 1-butene). Experimental evidence is consistent with the reaction likely being initiated by cationic [(^RPBP)Ni]⁺ species instead of Ni-alkyl/hydride complexes. Computational modeling suggests a unique mechanism that involves the formation of a 6-membered borametallacycle intermediate to be the most energetically feasible reaction pathway, and formation of this cyclic intermediate appears to involve cooperative ethylene activation by B and Ni. The PBP-Ni activation of ethylene and proposed mechanism appears to be unique for the conversion of ethylene to higher olefins.

Experimental Section

General information. All reactions were performed under a dinitrogen or argon atmosphere using Schlenk line techniques or inside a dinitrogen filled glovebox unless specified otherwise. GC-MS was performed using a Shimadzu GCMS-QP2020 NX with a 30 m × 0.25 mm Rt-Q-Bond capillary column with 8 μm film thickness and a 30 m × 0.25 mm Rxi-5ms capillary column with 0.25 μm film thickness using electron impact ionization method.

All NMR reactions were performed using Wilmad medium wall precision low pressure/vacuum (LPV) NMR tubes and pressurized with ethylene or propylene using a high-pressure line. Toluene was dried using a sodium-benzophenone/ketyl still under a dinitrogen atmosphere and stored inside a glovebox. Tetrahydrofuran and diethyl ether were dried via a potassium-benzophenone/ketyl still under a dinitrogen atmosphere and stored over activated 4Å molecular sieves inside a glovebox. Benzene, pentane, and methylene chloride were dried using a solvent purification system with activated alumina and stored under activated 3Å molecular sieves inside a dinitrogen filled glovebox. Hexanes was dried using 4Å molecular sieves. Toluene-*d*₈ and benzene-*d*₆ were dried and stored over activated 3Å molecular sieves inside a glovebox. Methylaluminoxane (MAO) used for the reaction was purchased from Sigma-Aldrich (MMAO-12, 7 wt. % Al in toluene). All other chemicals were purchased from commercial sources and used as received.

NMR spectra were recorded on Varian VNMRs 600 MHz or 500 MHz spectrometer or a Bruker Avance III 800 MHz spectrometer. All reported chemical shifts were referenced to residual ¹H resonances (¹H NMR) or ¹³C{¹H} resonances (¹³C{¹H} NMR). ¹H NMR: benzene-*d*₆ 7.16 ppm; toluene-*d*₈ 7.09 ppm. ¹³C NMR: benzene-*d*₆ 128.1 ppm; toluene-*d*₈ 137.5 ppm.⁷³ The ¹⁹F NMR spectra were referenced to hexafluorobenzene δ -164.9 ppm as an external standard. ³¹P{¹H} NMR spectra were referenced to H₃PO₄ δ 0.0 ppm as an external standard. Elemental analyses were performed by the University of Virginia Chemistry Department Elemental Analysis Facility.

General procedure for *in situ* ¹H NMR studies of ethylene dimerization. Described here is a representative procedure for our NMR studies. Inside a dry dinitrogen filled glovebox, a stock solution of internal standard hexamethyldisiloxane (HMDSO, 10 μL, 0.0471 mmol) in 10 mL of benzene-*d*₆ was made using a volumetric flask. A stock solution of Ni pre-catalyst (18.1 μmol) in

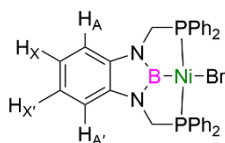
2 mL of the HMDSO/benzene- d_6 solution was made to ensure reproducible concentration of the Ni complex (9.05 mmol/L). The additive (18.1 μmol , 1 equiv. relative to Ni pre-catalyst) was added to the stock solution of Ni pre-catalyst. After stirring, 0.5 mL of the mixture was syringed into a medium-wall LPV NMR tubes. Then, the LPV NMR tubes were pressurized with 40 psig of ethylene. Quantitative ^1H NMR experiments were performed using HMDSO as the internal standard. The LPV NMR tube was held at room temperature or heated in an oil bath at a specific temperature, then the integration changes of the 1-butene, *trans*- and *cis*-2-butene signals were measured at time intervals by ^1H NMR experiments.

General procedure for high-pressure reactions under constant ethylene pressure. All high-pressure reactions were performed using customized steel reactors (VCO) with a fixed volume (300 cm^3) high pressure gas burette system. The connection between reactor and the gas burette system was custom built with the function to place all metal tubing under vacuum to prevent air or moisture contamination of the VCO reactor. The following is a representative procedure for our high-pressure studies. The high-pressure gas burette system was evacuated and refilled with pure ethylene (99.9%, 3.0 PL) using a high-pressure line. Inside a dry dinitrogen filled glovebox, the Ni pre-catalyst (9.05 μmol) was placed in the VCO reactor with a glass insert, followed by addition of dried toluene (1 mL total, the actual volume depends on the amount of additive used) and additives (equiv. relative to Ni pre-catalyst). When using lower Ni pre-catalyst loading, a stock solution of Ni pre-catalyst in dry toluene was made to ensure reproducible concentrations of Ni complex. Then the VCO reactor was sealed and connected to the high-pressure gas burette system prefilled with ethylene. The connection metal tubing was evacuated and then charged with ethylene, and this process was repeated three times. The output ethylene pressure was set to 200 psig (or 600 psig under some conditions). Then the valve connected to the

VCO reactor was opened, and the pressure on the gas burette was recorded. After specific reaction time (10 or 20 min), the valve connected to the VCO reactor was closed and the pressure on the gas burette was recorded, followed by placing the VCO reactor into a dry ice/acetone bath. The pressure change of the gas burette was used to calculate ethylene consumption using the ideal gas law. After the reactor was sufficiently cooled, the top pressure was slowly released, followed by adding 1 mL of toluene (undried) to the reactor. For the conditions using 1000 equivalents of alkylaluminum, 1 drop of water was added. Then, 50 μL of tetrahydrofuran were syringed into the reactor as the standard for GC-MS analysis. Butenes were quantified using a Rt-Q-Bond column, and the remainder of the olefins was quantified using with a Rxi-5ms column.

Synthesis and characterization of Ni complexes. ($^t\text{BuPBP}$)NiOAc (**1**),⁴⁹ and ($^t\text{BuPBP}$)NiBr (**2**),⁵⁰ and ($^{\text{Ph}}\text{PBP}$)H³³ were synthesized based on published procedures.

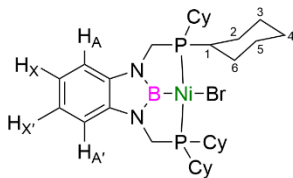
($^{\text{Ph}}\text{PBP}$)NiBr (3). To a solution of (DME)NiBr₂ (240 mg, 0.778 mmol) in 15 mL of dry toluene under Ar atmosphere, a solution of ($^{\text{Ph}}\text{PBP}$)H (400 mg, 0.778 mmol) and Et₃N (0.24 mL, 1.556 mmol) in 15 mL of dry toluene was cannulated slowly at $-78\text{ }^{\circ}\text{C}$. The reaction mixture was allowed to warm to room temperature slowly and stirred overnight. The solvent was removed *in vacuo*, then the solid residue was washed with cold pentane ($-20\text{ }^{\circ}\text{C}$, 5 mL \times 2). The resulting solid was extracted using dry toluene, and the solution was dried under vacuum to isolate the product as an orange-yellow solid that is sensitive to moisture and oxygen (390 mg, 78% isolated yield).



¹H NMR (800 MHz, benzene-*d*₆) δ 7.89 (dd vt, ¹*J*_{H,H} = 7 Hz, ³*J*_{H,H} = 2 Hz, 8H), 7.15 (AA'XX' dd, partially overlapped with benzene-*d*₆, 2H), 7.01 – 6.96 (m, 12H), 6.90 (AA'XX' dd, *J*_{AX} = 7.7

Hz, $J_{AX'} = 1.2$ Hz, $J_{AA'} = 0.4$ Hz, $J_{XX'} = 7.6$ Hz, 2H), 4.00 (vt, $N = 4.8$ Hz, 4H, NCH_2P). $^{31}P\{^1H\}$ NMR (243 MHz, benzene- d_6) δ 47.26 (s). $^{13}C\{^1H\}$ NMR (201 MHz, benzene- d_6) δ 139.2 (vt, $N = 18$ Hz), 133.7 (vt, $N = 12$ Hz), 132.7 (vt, $N = 38$ Hz), 130.4, 128.8 (vt, $N = 9$ Hz), 119.4, 109.7, 49.1 (vt, $N = 44$ Hz, PCH_2). Anal. Calcd for $C_{32}H_{28}BBrN_2NiP_2$: C, 58.95; H, 4.33; N, 4.30. Found: C, 58.89; H, 4.50; N, 4.18.

(^{Cy}PBP)NiBr (4). A solution of (^{Cy}PBP)H ligand (500 mg, 0.928 mmol) in toluene (10 mL) and Et_3N (0.285 mL, 2.04 mmol) at -20 °C was transferred via cannula to a suspension of (DME)NiBr₂ (286.4 mg, 0.928 mmol) in toluene (10 mL) at the same temperature. The resulting suspension was allowed to warm to room temperature, and it was stirred at the same temperature for 18 h, after which the stirring was stopped, and the dark yellow solution decanted to a Schlenk flask by using a cannula with a double filter paper. The remaining solid was extracted with toluene (10 mL \times 3), and the combined organic phase was evaporated under vacuum to give Ni–Br as a brown solid (578 mg, 0.854 mmol, 92% yield). X-Ray quality crystals can be obtained by diffusion of pentane into a toluene solution of **4**.



1H NMR (400 MHz, benzene- d_6): δ 7.18 (AA'XX' dd, partially overlapped with benzene- d_6 , 2H, aromatic CH), 7.01 (AA'XX' dd, $J_{AX} = 7.6$ Hz, $J_{AX'} = 1.3$ Hz, $J_{AA'} = 0.5$ Hz, $J_{XX'} = 7.6$ Hz, 2H, aromatic CH), 3.41 (vt, $N = 4.2$ Hz, 4H, NCH_2P), 2.30 (m, 4 H, CH_2), 2.19 (quint vt, $^3J_{HH} = 2.9$ Hz, $N = 24.6$ Hz, 4H, $CH-P$), 1.80 (m, 4 H, CH_2), 1.70 (m, 4 H, CH_2), 1.59 (m, 12 H, CH_2), 1.36 (m, 4 H, CH_2), 1.22 (m, 4 H, CH_2), 1.08 (m, 8 H, CH_2). $^{31}P\{^1H\}$ NMR (161 MHz, benzene- d_6) δ 66.68 (s). $^{11}B\{^1H\}$ NMR (128 MHz, benzene- d_6): δ 40.3 (br s, boryl). $^{13}C\{^1H\}$ NMR (100 MHz,

benzene-*d*₆): δ 139.7 (vt, $N = 16$ Hz, ligand aromatic C_q), 119.0 (ligand aromatic CH), 109.3 (ligand aromatic CH), 40.5 (vt, $N = 37$ Hz, NCH₂P), 33.9 (vt, $N = 19$. Hz, C₁), 29.2 (C₂, C₆), 28.8, 27.1 – 27.3 (m, C₃, C₅), 26.5 (C₄). Anal. Calcd. for C₃₂H₅₂BBrN₂NiP₂: C, 56.85; H, 7.75; N, 4.14. Found: C, 56.65; H, 8.03; N, 4.26.

Associated Content

Supporting Information

The Supporting Information is available free of charge.

Additional experimental procedures and details, additional condition screening results, control experiments, GC methods and representative chromatograms, NMR and HRMS spectra of the complexes, crystal structure data (PDF).

Computational details, Cartesian coordinates for the calculated structures and absolute energies.

Access Codes

CCDC 2203706–2203708, and 2212008 contains the supplementary crystallographic data for this paper. These data can be obtained free of charge via www.ccdc.cam.ac.uk/structures.

Author Information

Corresponding Authors

T. Brent Gunnoe – Department of Chemistry, University of Virginia, Charlottesville, Virginia 22904, United States; orcid.org/0000-0001-5714-3887; Email: tbg7h@virginia.edu

Amor Rodríguez – Instituto de Investigaciones Químicas (IIQ), Department of Inorganic Chemistry CSIC and. University of Seville, Center for Innovation in Advanced Chemistry (ORFEO-CINQA), C/Américo Vespucio 49, Seville, 41092, Spain; orcid.org/0000-0001-9194-5613; Email: marodriguez@iiq.csic.es

Authors

Fanji Kong – Department of Chemistry, University of Virginia, Charlottesville, Virginia 22904, United States; orcid.org/0000-0003-4136-1403

Pablo Ríos – Instituto de Investigaciones Químicas (IIQ), Department of Inorganic Chemistry CSIC and. University of Seville, Center for Innovation in Advanced Chemistry (ORFEO-CINQA), C/Américo Vespucio 49, Seville, 41092, Spain; orcid.org/0000-0003-4467-4157

Conner Hauck – Department of Chemistry, University of Virginia, Charlottesville, Virginia 22904, United States; orcid.org/0000-0003-4136-1403

Francisco José Fernández-de-Córdova – Instituto de Investigaciones Químicas (IIQ), Department of Inorganic Chemistry CSIC and. University of Seville, Center for Innovation in Advanced Chemistry (ORFEO-CINQA), C/Américo Vespucio 49, Seville, 41092, Spain; orcid.org/0000-0002-1784-2840

Diane A. Dickie – Department of Chemistry, University of Virginia, Charlottesville, Virginia 22904, United States; orcid.org/0000-0003-0939-3309

Laurel G. Habgood – Department of Chemistry, Rollins College, Winter Park, Florida 32789, United States; orcid.org/0000-0001-5475-1561

Acknowledgment

The U.S. National Science Foundation (CHE-2102433) provided support for the experimental efforts. Single crystal X-ray diffraction experiments were performed on a diffractometer at the University of Virginia funded by the NSF-MRI program (CHE-2018870). Financial support (FEDER contribution) for the computational studies was provided from the MINECO (Projects PID2019 109312GB-IOO and RED2018-102387-T), Junta de Andalucía (Project PY20_00513) and the CSIC (AEPP-CTQ2016-76267-P).

References

1. Pillai, S. M.; Ravindranathan, M.; Sivaram, S., Dimerization of ethylene and propylene catalyzed by transition-metal complexes. *Chem. Rev.* **1986**, *86*, 353-399. doi: 10.1021/cr00072a004
2. Olivier-Bourbigou, H.; Breuil, P. A. R.; Magna, L.; Michel, T.; Espada Pastor, M. F.; Delcroix, D., Nickel Catalyzed Olefin Oligomerization and Dimerization. *Chem. Rev.* **2020**, *120*, 7919-7983. doi: 10.1021/acs.chemrev.0c00076
3. Ittel, S. D.; Johnson, L. K.; Brookhart, M., Late-Metal Catalysts for Ethylene Homo- and Copolymerization. *Chem. Rev.* **2000**, *100*, 1169-1204. doi: 10.1021/cr9804644
4. Bekmukhamedov, G. E.; Sukhov, A. V.; Kuchkaev, A. M.; Yakhvarov, D. G., Ni-Based Complexes in Selective Ethylene Oligomerization Processes. *Catalysts* **2020**, *10*, 498. doi: 10.3390/catal10050498

5. Breuil, P.-A. R.; Magna, L.; Olivier-Bourbigou, H., Role of Homogeneous Catalysis in Oligomerization of Olefins : Focus on Selected Examples Based on Group 4 to Group 10 Transition Metal Complexes. *Catal. Lett.* **2015**, *145*, 173-192. doi: 10.1007/s10562-014-1451-x
6. S&P Global's Linear Alpha-Olefins Chemical Economics Handbook (CEH). <https://www.spglobal.com/commodityinsights/en/ci/products/linear-alpha-olefins-chemical-economics-handbook.html> (accessed 2022-08-31).
7. Ziegler, K.; Gellert, H.; Holzkamp, E.; Wilke, G., Entdeckung des Nickel Effekts. *Brennst.-Chem.* **1954**, *35*, 321.
8. Fischer, K.; Jonas, K.; Misbach, P.; Stabba, R.; Wilke, G., The "Nickel Effect". *Angew. Chem. Int. Ed.* **1973**, *12*, 943-953. doi: 10.1002/anie.197309431
9. McGuinness, D. S., Olefin Oligomerization via Metallacycles: Dimerization, Trimerization, Tetramerization, and Beyond. *Chem. Rev.* **2011**, *111*, 2321-2341. doi: 10.1021/cr100217q
10. Sydora, O. L., Selective Ethylene Oligomerization. *Organometallics* **2019**, *38*, 997-1010. doi: 10.1021/acs.organomet.8b00799
11. Keim, W.; Kowaldt, F. H.; Goddard, R.; Krüger, C., Novel Coordination of (Benzoylmethylene)triphenylphosphorane in a Nickel Oligomerization Catalyst. *Angew. Chem. Int. Ed.* **1978**, *17*, 466-467. doi: 10.1002/anie.197804661
12. Kuhn, P.; Sémeril, D.; Matt, D.; Chetcuti, M. J.; Lutz, P., Structure–reactivity relationships in SHOP-type complexes: tunable catalysts for the oligomerisation and polymerisation of ethylene. *Dalton Trans.* **2007**, 515-528. doi: 10.1039/B615259G

13. Keim, W., Oligomerization of Ethylene to α -Olefins: Discovery and Development of the Shell Higher Olefin Process (SHOP). *Angew. Chem. Int. Ed.* **2013**, *52*, 12492-12496. doi: 10.1002/anie.201305308
14. Speiser, F.; Braunstein, P.; Saussine, L., Catalytic Ethylene Dimerization and Oligomerization: Recent Developments with Nickel Complexes Containing P,N-Chelating Ligands. *Acc. Chem. Res.* **2005**, *38*, 784-793. doi: 10.1021/ar050040d
15. Cossee, P., Ziegler-Natta catalysis I. Mechanism of polymerization of α -olefins with Ziegler-Natta catalysts. *J. Catal.* **1964**, *3*, 80-88. doi: 10.1016/0021-9517(64)90095-8
16. Flory, P. J., Molecular Size Distribution in Linear Condensation Polymers¹. *J. Am. Chem. Soc.* **1936**, *58*, 1877-1885. doi: 10.1021/ja01301a016
17. Schulz, P. A.; Sudbø, A. S.; Krajnovich, D. J.; Kwok, H. S.; Shen, Y. R.; Lee, Y. T., Multiphoton Dissociation of Polyatomic Molecules. *Annu. Rev. Phys. Chem.* **1979**, *30*, 379-409. doi: 10.1146/annurev.pc.30.100179.002115
18. Britovsek, G. J. P.; Malinowski, R.; McGuinness, D. S.; Nobbs, J. D.; Tomov, A. K.; Wadsley, A. W.; Young, C. T., Ethylene Oligomerization beyond Schulz–Flory Distributions. *ACS Catal.* **2015**, *5*, 6922-6925. doi: 10.1021/acscatal.5b02203
19. Overett, M. J.; Blann, K.; Bollmann, A.; Dixon, J. T.; Haasbroek, D.; Killian, E.; Maumela, H.; McGuinness, D. S.; Morgan, D. H., Mechanistic Investigations of the Ethylene Tetramerisation Reaction. *J. Am. Chem. Soc.* **2005**, *127*, 10723-10730. doi: 10.1021/ja052327b
20. Titova, Y. Y.; Belykh, L. B.; Rokhin, A. V.; Soroka, O. G.; Schmidt, F. K., Catalysis of dimerization and oligomerization reactions of lower alkenes by systems based on Ni(PPh₃)₂(C₂H₄) and Ni(PPh₃)_nCl (n = 2 or 3). *Kinet. Catal.* **2014**, *55*, 35-46. doi: 10.1134/S0023158414010169

21. Bernardi, F.; Bottoni, A.; Rossi, I., A DFT Investigation of Ethylene Dimerization Catalyzed by Ni(0) Complexes. *J. Am. Chem. Soc.* **1998**, *120*, 7770-7775. doi: 10.1021/ja980604r
22. Grubbs, R. H.; Miyashita, A., The metallacyclopentane–olefin interchange reaction. *J. Chem. Soc., Chem. Commun.* **1977**, 864-865. doi: 10.1039/c39770000864
23. Grubbs, R. H.; Miyashita, A.; Liu, M.-I. M.; Burk, P. L., The preparation and reactions of nickelocyclopentanes. *J. Am. Chem. Soc.* **1977**, *99*, 3863-3864. doi: 10.1021/ja00453a068
24. Grubbs, R. H.; Miyashita, A., Metallacyclopentanes as catalysts for the linear and cyclodimerization of olefins. *J. Am. Chem. Soc.* **1978**, *100*, 7416-7418. doi: 10.1021/ja00491a051
25. Grubbs, R. H.; Miyashita, A., The relationship between metallacyclopentanes and bis(olefin)-metal complexes. *J. Am. Chem. Soc.* **1978**, *100*, 1300-1302. doi: 10.1021/ja00472a050
26. Grubbs, R. H.; Miyashita, A.; Liu, M.; Burk, P., Preparation and reactions of phosphine nickelocyclopentanes. *J. Am. Chem. Soc.* **1978**, *100*, 2418-2425. doi: 10.1021/ja00476a026
27. Gu, S.; Nielsen, R. J.; Taylor, K. H.; Fortman, G. C.; Chen, J.; Dickie, D. A.; Goddard, W. A.; Gunnoe, T. B., Use of Ligand Steric Properties to Control the Thermodynamics and Kinetics of Oxidative Addition and Reductive Elimination with Pincer-Ligated Rh Complexes. *Organometallics* **2020**, *39*, 1917-1933. doi: 10.1021/acs.organomet.0c00122
28. Kong, F.; Gu, S.; Liu, C.; Dickie, D. A.; Zhang, S.; Gunnoe, T. B., Effects of Additives on Catalytic Arene C–H Activation: Study of Rh Catalysts Supported by Bis-phosphine Pincer Ligands. *Organometallics* **2020**, *39*, 3918-3935. doi: 10.1021/acs.organomet.0c00623
29. Goldberg, J. M.; Wong, G. W.; Brastow, K. E.; Kaminsky, W.; Goldberg, K. I.; Heinekey, D. M., The Importance of Steric Factors in Iridium Pincer Complexes. *Organometallics* **2015**, *34*, 753-762. doi: 10.1021/om501166w

30. Arora, V.; Narjinari, H.; Nandi, P. G.; Kumar, A., Recent advances in pincer–nickel catalyzed reactions. *Dalton Trans.* **2021**, *50*, 3394-3428. doi: 10.1039/d0dt03593a
31. Segawa, Y.; Yamashita, M.; Nozaki, K., Boryllithium: Isolation, Characterization, and Reactivity as a Boryl Anion. *Science* **2006**, *314*, 113. doi: 10.1126/science.1131914
32. Segawa, Y.; Yamashita, M.; Nozaki, K., Syntheses of PBP Pincer Iridium Complexes: A Supporting Boryl Ligand. *J. Am. Chem. Soc.* **2009**, *131*, 9201-9203. doi: 10.1021/ja9037092
33. Segawa, Y.; Yamashita, M.; Nozaki, K., Diphenylphosphino- or Dicyclohexylphosphino-Tethered Boryl Pincer Ligands: Syntheses of PBP Iridium(III) Complexes and Their Conversion to Iridium–Ethylene Complexes. *Organometallics* **2009**, *28*, 6234-6242. doi: 10.1021/om9006455
34. Hill, A. F.; Lee, S. B.; Park, J.; Shang, R.; Willis, A. C., Analogies between Metallaboratranes, Triboronates, and Boron Pincer Ligand Complexes. *Organometallics* **2010**, *29*, 5661-5669. doi: 10.1021/om100557q
35. Ogawa, H.; Yamashita, M., Trial for anti-Markovnikov Hydration of 1-Decene Using Platinum Complexes Bearing a PBP Pincer Ligand, Inducing Alkene Isomerization and Decomposition of PBP Ligand. *Chem. Lett.* **2014**, *43*, 664-666. doi: 10.1246/cl.131208
36. McQueen, C. M. A.; Hill, A. F.; Sharma, M.; Singh, S. K.; Ward, J. S.; Willis, A. C.; Young, R. D., Synthesis and reactivity of osmium and ruthenium PBP–LXL boryl pincer complexes. *Polyhedron* **2016**, *120*, 185-195. doi: 10.1016/j.poly.2016.05.041
37. Ogawa, H.; Yamashita, M., Platinum complexes bearing a boron-based PBP pincer ligand: synthesis, structure, and application as a catalyst for hydrosilylation of 1-decene. *Dalton Trans.* **2013**, *42*, 625-629. doi: 10.1039/c2dt31892j

38. Hasegawa, M.; Segawa, Y.; Yamashita, M.; Nozaki, K., Isolation of a PBP-Pincer Rhodium Complex Stabilized by an Intermolecular C---H σ Coordination as the Fourth Ligand. *Angew. Chem. Int. Ed.* **2012**, *51*, 6956-6960. doi: doi:10.1002/anie.201201916
39. Fang, F.; Xue, M. M.; Ding, M.; Zhang, J.; Li, S.; Chen, X., The Stability of Diphosphino-Boryl PBP Pincer Backbone: PBP to POP Ligand Hydrolysis. *Chemistry – An Asian Journal* **2021**, *16*, 2489-2494. doi: 10.1002/asia.202100690
40. Lin, T.-P.; Peters, J. C., Boryl-Mediated Reversible H₂ Activation at Cobalt: Catalytic Hydrogenation, Dehydrogenation, and Transfer Hydrogenation. *J. Am. Chem. Soc.* **2013**, *135*, 15310-15313. doi: 10.1021/ja408397v
41. Ding, Y.; Ma, Q.-Q.; Kang, J.; Zhang, J.; Li, S.; Chen, X., Palladium(II) complexes supported by PBP and POCOP pincer ligands: a comparison of their structure, properties and catalytic activity. *Dalton Trans.* **2019**, *48*, 17633-17643. doi: 10.1039/c9dt03954f
42. Tanoue, K.; Yamashita, M., Synthesis of Pincer Iridium Complexes Bearing a Boron Atom and ⁱPr-Substituted Phosphorus Atoms: Application to Catalytic Transfer Dehydrogenation of Alkanes. *Organometallics* **2015**, *34*, 4011-4017. doi: 10.1021/acs.organomet.5b00376
43. Hill, A. F.; McQueen, C. M. A., Arrested B–H Activation en Route to Installation of a PBP Pincer Ligand on Ruthenium and Osmium. *Organometallics* **2014**, *33*, 1977-1985. doi: 10.1021/om5001106
44. Miyada, T.; Yamashita, M., Oxygenation of a Ruthenium Complex Bearing a PBP-Pincer Ligand Inducing the Formation of a Boronato Ligand with a Weak Ru–O Bond. *Organometallics* **2013**, *32*, 5281-5284. doi: 10.1021/om400915x

45. Hayashi, S.; Murayama, T.; Kusumoto, S.; Nozaki, K., Pincer - Supported Perfluororhodacyclopentanes: High Nucleophilicity of the M–C^F Bond. *Angew. Chem. Int. Ed.* **2022**, *61*, e202207760. doi: 10.1002/anie.202207760
46. Lin, T.-P.; Peters, J. C., Boryl–Metal Bonds Facilitate Cobalt/Nickel-Catalyzed Olefin Hydrogenation. *J. Am. Chem. Soc.* **2014**, *136*, 13672-13683. doi: 10.1021/ja504667f
47. Ríos, P.; Curado, N.; López-Serrano, J.; Rodríguez, A., Selective reduction of carbon dioxide to bis(silyl)acetal catalyzed by a PBP-supported nickel complex. *Chem. Commun.* **2016**, *52*, 2114-2117. doi: 10.1039/C5CC09650B
48. Ríos, P.; Rodríguez, A.; López-Serrano, J., Mechanistic Studies on the Selective Reduction of CO₂ to the Aldehyde Level by a Bis(phosphino)boryl (PBP)-Supported Nickel Complex. *ACS Catal.* **2016**, *6*, 5715-5723. doi: 10.1021/acscatal.6b01715
49. Deziel, A. P.; Espinosa, M. R.; Pavlovic, L.; Charboneau, D. J.; Hazari, N.; Hopmann, K. H.; Mercado, B. Q., Ligand and solvent effects on CO₂ insertion into group 10 metal alkyl bonds. *Chem. Sci.* **2022**, *13*, 2391-2404. doi: 10.1039/d1sc06346d
50. Curado, N.; Maya, C.; López-Serrano, J.; Rodríguez, A., Boryl-assisted hydrogenolysis of a nickel–methyl bond. *Chem. Commun.* **2014**, *50*, 15718-15721. doi: 10.1039/C4CC07616H
51. Seidel, F. W.; Nozaki, K., A Ni⁰ σ -Borane Complex Bearing a Rigid Bidentate Borane/Phosphine Ligand: Boryl Complex Formation by Oxidative Dehydrochloroborylation and Catalytic Activity for Ethylene Polymerization. *Angew. Chem. Int. Ed.* **2022**, *61*, e202111691. doi: 10.1002/anie.202111691

52. Fontaine, F.-G.; Zargarian, D., $\text{Me}_2\text{AlCH}_2\text{PMe}_2$: A New, Bifunctional Cocatalyst for the Ni(II)-Catalyzed Oligomerization of PhSiH_3 . *J. Am. Chem. Soc.* **2004**, *126*, 8786-8794. doi: 10.1021/ja048911m
53. Chandran, D.; Byeon, S. J.; Suh, H.; Kim, I., Effect of Ion-Pair Strength on Ethylene Oligomerization by Divalent Nickel Complexes. *Catal. Lett.* **2013**, *143*, 717-722. doi: 10.1007/s10562-013-1021-7
54. Dresch, L. C.; de Araújo, B. B.; Casagrande, O. d. L.; Stieler, R., A novel class of nickel(ii) complexes containing selenium-based bidentate ligands applied in ethylene oligomerization. *RSC Advances* **2016**, *6*, 104338-104344. doi: 10.1039/C6RA18987C
55. Huang, Y.; Zhang, L.; Wei, W.; Alam, F.; Jiang, T., Nickel-based ethylene oligomerization catalysts supported by PNSiP ligands. *Phosphorus, Sulfur Silicon Relat. Elem.* **2018**, *193*, 363-368. doi: 10.1080/10426507.2018.1424157
56. Xu, C.; Shen, Q.; Sun, X.; Tang, Y., Synthesis, Characterization, and Highly Selective Ethylene Dimerization to 1-Butene of $[\text{O}-\text{NX}]\text{Ni}(\text{II})$ Complexes. *Chin. J. Chem.* **2012**, *30*, 1105-1113. doi: 10.1002/cjoc.201100443
57. Ziegler, K., Aluminium-organische Synthese im Bereich olefinischer Kohlenwasserstoffe. *Angew. Chem.* **1952**, *64*, 323-329. doi: 10.1002/ange.19520641202
58. Holah, D. G.; Hughes, A. N.; Hui, B. C.; Kan, C.-T., Production of Ni(I) complexes from reactions between Ni(II) and NaBH_4 in the presence of triphenylphosphine and some bidentate phosphines. *Can. J. Chem.* **1978**, *56*, 2552-2559. doi: 10.1139/v78-419
59. Chandran, D.; Lee, K. M.; Chang, H. C.; Song, G. Y.; Lee, J.-E.; Suh, H.; Kim, I., Ni(II) complexes with ligands derived from phenylpyridine, active for selective dimerization and

trimerization of ethylene. *J. Organomet. Chem.* **2012**, *718*, 8-13. doi: 10.1016/j.jorganchem.2012.08.005

60. Zhang, M.; Zhang, S.; Hao, P.; Jie, S.; Sun, W.-H.; Li, P.; Lu, X., Nickel Complexes Bearing 2-(Benzimidazol-2-yl)-1,10-phenanthrolines: Synthesis, Characterization and Their Catalytic Behavior Toward Ethylene Oligomerization. *Eur. J. Inorg. Chem.* **2007**, *2007*, 3816-3826. doi: 10.1002/ejic.200700392

61. Antonov, A. A.; Semikolenova, N. V.; Soshnikov, I. E.; Talsi, E. P.; Bryliakov, K. P., Selective Ethylene Dimerization into 2-Butenes Using Homogeneous and Supported Nickel(II) 2-Iminopyridine Catalysts. *Top. Catal.* **2020**, *63*, 222-228. doi: 10.1007/s11244-019-01208-8

62. Boudier, A.; Breuil, P.-A. R.; Magna, L.; Olivier-Bourbigou, H.; Braunstein, P., Nickel(II) complexes with imino-imidazole chelating ligands bearing pendant donor groups (SR, OR, NR₂, PR₂) as precatalysts in ethylene oligomerization. *J. Organomet. Chem.* **2012**, *718*, 31-37. doi: 10.1016/j.jorganchem.2012.07.044

63. Feng, C.; Zhou, S.; Wang, D.; Zhao, Y.; Liu, S.; Li, Z.; Braunstein, P., Cooperativity in Highly Active Ethylene Dimerization by Dinuclear Nickel Complexes Bearing a Bifunctional PN Ligand. *Organometallics* **2021**, *40*, 184-193. doi: 10.1021/acs.organomet.0c00683

64. Haghverdi, M.; Tadjarodi, A.; Bahri-Laleh, N.; Nekoomanesh-Haghighi, M., Synthesis and characterization of Ni(II) complexes bearing of 2 - (1*H*-benzimidazol - 2 - yl) - phenol derivatives as highly active catalysts for ethylene oligomerization. *Appl. Organomet. Chem.* **2018**, *32*, e4015. doi: 10.1002/aoc.4015

65. Mukherjee, S.; Patel, B. A.; Bhaduri, S., Selective Ethylene Oligomerization with Nickel Oxime Complexes. *Organometallics* **2009**, *28*, 3074-3078. doi: 10.1021/om900080h

66. Gutsulyak, D. V.; Gott, A. L.; Piers, W. E.; Parvez, M., Dimerization of Ethylene by Nickel Phosphino–Borate Complexes. *Organometallics* **2013**, *32*, 3363-3370. doi: 10.1021/om400288u
67. Boulens, P.; Pellier, E.; Jeanneau, E.; Reek, J. N. H.; Olivier-Bourbigou, H.; Breuil, P.-A. R., Self-Assembled Organometallic Nickel Complexes as Catalysts for Selective Dimerization of Ethylene into 1-Butene. *Organometallics* **2015**, *34*, 1139-1142. doi: 10.1021/acs.organomet.5b00055
68. The transition state observed for S=0 (singlet state) is 49.0 kcal mol⁻¹. Nonetheless, the diradical species (S=1) was also considered, as described in reference 21. However, this barrier was even higher in Gibbs free energy (83.4 kcal mol⁻¹).
69. Ríos, P.; Borge, J.; Fernández De Córdova, F.; Sciortino, G.; Lledós, A.; Rodríguez, A., Ambiphilic boryl groups in a neutral Ni(II) complex: a new activation mode of H₂. *Chem. Sci.* **2021**, *12*, 2540-2548. doi: 10.1039/d0sc06014c
70. He, T.; Tsvetkov, N. P.; Andino, J. G.; Gao, X.; Fullmer, B. C.; Caulton, K. G., Mechanism of Heterolysis of H₂ by an Unsaturated d⁸ Nickel Center: via Tetravalent Nickel? *J. Am. Chem. Soc.* **2010**, *132*, 910-911. doi: 10.1021/ja908674x
71. Craig, N. C.; Groner, P.; McKean, D. C., Equilibrium Structures for Butadiene and Ethylene: Compelling Evidence for Π -Electron Delocalization in Butadiene. *J. Phys. Chem. A.* **2006**, *110*, 7461-7469. doi: 10.1021/jp060695b
72. Brookhart, M.; Green, M. L. H.; Parkin, G., Agostic interactions in transition metal compounds. *Proc. Natl. Acad. Sci. U. S. A.* **2007**, *104*, 6908-6914. doi: 10.1073/pnas.0610747104
73. Fulmer, G. R.; Miller, A. J. M.; Sherden, N. H.; Gottlieb, H. E.; Nudelman, A.; Stoltz, B. M.; Bercaw, J. E.; Goldberg, K. I., NMR Chemical Shifts of Trace Impurities: Common

Laboratory Solvents, Organics, and Gases in Deuterated Solvents Relevant to the Organometallic
Chemist. *Organometallics* **2010**, 29, 2176-2179. doi: 10.1021/om100106e

TOC Graphic

